spectrum

SuperCOSMOS Comes into Operation

DECEMBER 1994

ISSUE NO. 4

NEWSLETTER OF THE
ROYAL OBSERVATORIES

The Royal Observatories

PPARC

Particle Physics and Astronomy Research Council

Royal Greenwich Observatory
Madingley Road
Cambridge CB3 0EZ
England

tel: +44 223 374000
fax: +44 223 374700
internet: **<user>@mail.ast.cam.ac.uk**

Royal Observatory Edinburgh
Blackford Hill
Edinburgh EH9 3HJ
Scotland

tel: +44 31 668 8100
fax: +44 31 662 1668
internet: **<user>@roe.ac.uk**

Isaac Newton Group of Telescopes
Royal Greenwich Observatory
Apartado de Correos 321
38780 Santa Cruz de La Palma
Tenerife
Islas Canarias

tel: +34 22 405500
fax (INT): +34 22 405646
SPAN: **29146::<user>**
internet: **<user>@lpve.ing.iac.es**

Joint Astronomy Centre
660 N. A'Ohoku Place
University Park
Hilo
Hawaii 96720
USA

tel: +1 808 961 3756
answerphone: +1 808 935 4332
fax: +1 808 961 6516
PSS: 315280809053
internet: **<user>@jach.hawaii.edu**

JAC Offices at Hale Pohaku: +1 808 935 9911
JCMT Carousel: +1 808 935 0852
UKIRT Dome: +1 808 961 6091
fax (JCMT): +1 808 935 5493

ING User Manuals: copies may be obtained by contacting Bill Martin at RGO (username **wlm**).

JCMT User Guide: copies may be obtained by contacting Dorothy Skedd at ROE (username **dacs**) or Henry Matthews at JAC (username **hem**).

UKIRT User Manual: copies may be obtained by contacting Dorothy Skedd at ROE (username **dacs**).

UKST User Manuals: copies can be obtained by contacting the UK Schmidt Telescope Unit at ROE (username **ukstu**).

ING on-line documentation (the LPINFO system) is available from a captive account **inginfo** on the RGO VAX **gxvg.ast.cam.ac.uk**, accessible by remote login; also available via World Wide Web URL **http:// ing.iac.es**.

JCMT on-line documentation is available from a FILESERV system (**jcmt_info@jach.hawaii.edu**) accessible at the JAC via e-mail and via World Wide Web URL **http:// www.jach.hawaii.edu/JCMT/index.html**.

UKIRT on-line documentation (the UKIRT_INFORM system) is available via World Wide Web URL **http:// www.jach.hawaii.edu/UKIRT/home.html**.

ING service observing: applications should be sent by e-mail to **service@mail.ast.cam.ac.uk** or **service@ing.iac.es**.

JCMT service observing: applications should be sent by e-mail to **jcmtserv@roe.ac.uk**.

UKIRT service observing: applications should be sent by e-mail to **ukirtserv@roe.ac.uk** or **ukirtserv@jach.hawaii.edu**.

UKST photography: applications for new plates (and loans from the Plate Library) should be sent to the UK Schmidt Telescope Unit at ROE. Forms can be obtained from UKSTU and may be submitted at any time.

Spectrum editors: Mark Holmes (username spectrum) and Keith Tritton (username kpt) at RGO and Mark Casali (username mmc) at ROE.

ISSN 1353–7784

contents

features

news

spectrum is published quarterly in March, June, September and December by the Royal Observatories

Measuring the Size and Age of the Universe

The RGO was inundated in the last week of October with radio and TV crews, all eager to get a simple explanation of the implications of the most accurate measurement yet of the distance of the Virgo galaxy M100. This measurement was recently made by the Hubble Space Telescope (HST) Key Project dedicated to determining the extragalactic distance scale (*ie* to measure the value of the Hubble constant, H_0). Most of the team are in the USA, Australia and Canada, but they now also have a member at the RGO.

Although the team is only in the first phase of a major systematic programme to measure accurately the scale, size, and age of the universe, a firm distance to the Virgo cluster is a critical milestone for the extragalactic distance scale and it has major implications for the Hubble constant.

HST has made the most accurate measurements yet of the distance to the Virgo cluster galaxy M100.

Using HST the team has detected 20 Cepheid variable stars in the spiral galaxy M100, a member of the Virgo cluster, which establishes the distance to the cluster to be 17.1 ± 1.8 Mpc (51 million light-years). This makes M100 the most distant galaxy in which Cepheid variables have been measured. Making the assumption that M100 lies at the mean distance of the Virgo cluster of galaxies gives a value for H_0 of 80 ± 17km/sec/Mpc. These results were published in the October 27 issue of the journal *Nature*.

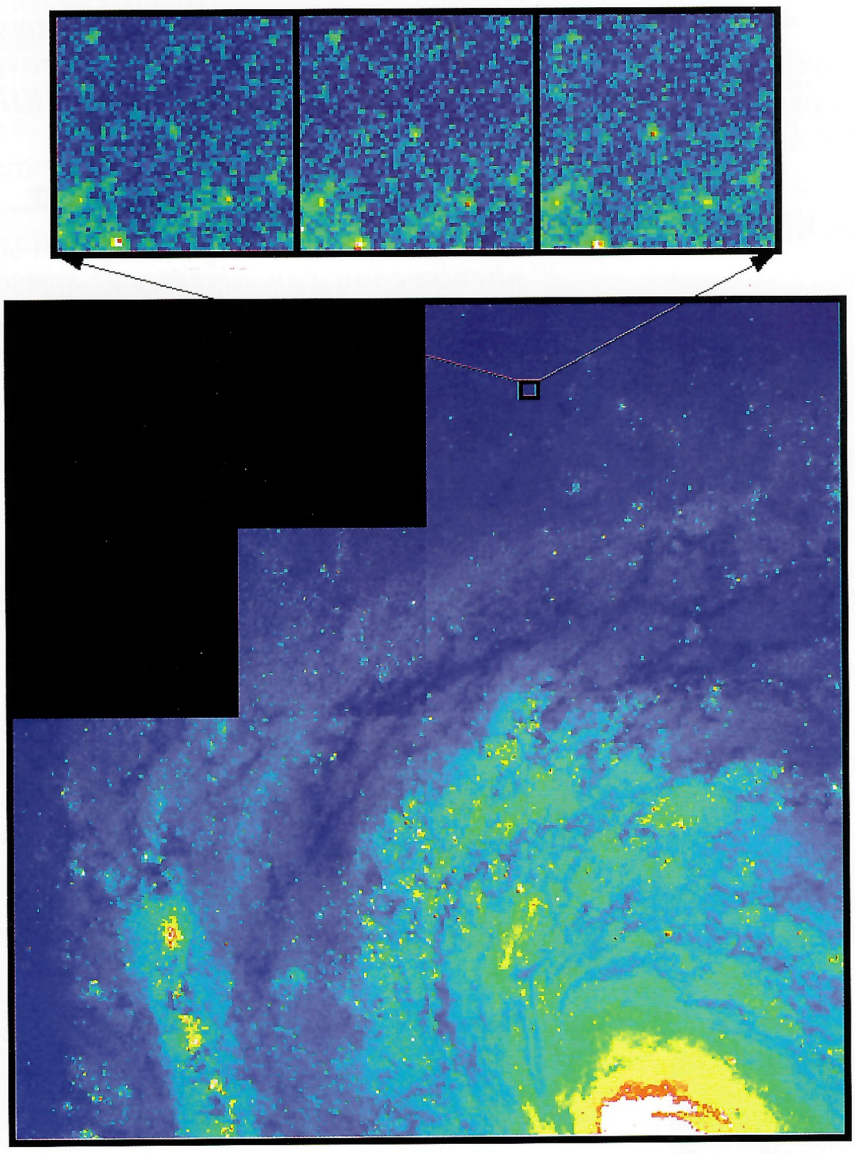

Fig. 1 – The sequence of images in the upper panel, taken with NASA's Hubble Space Telescope, shows the rhythmic changes in a Cepheid variable located in the Virgo cluster galaxy M100. This Cepheid has a magnitude amplitude of V = 24.5 to 25.3 and a period of 51.3 days.

Most of the quoted error in the value of H_0 is due to the uncertainty in the position of M100 with respect to the rest of the Virgo galaxies. Hence the next step will be to measure Virgo's distance more accurately by obtaining the Cepheid distances to a further 2 Virgo galaxies. However, because Virgo also has a large velocity dispersion, the final value for H_0 won't be determined until the team's entire programme has been completed (in 2 – 3 years), as this involves the calibration of several secondary distance indicators which will then be capable of measuring accurate distances to galaxies well beyond Virgo, and hence to regions where local velocity perturbations will be small compared to their Hubble flow.

Standard theory

Much of the fuss over this value for H_0, derived from the distance to M100, is due to the age of the Universe derived from the standard theory of cosmology of just 8 billion years. This is about half the age of the oldest stars in our galaxy. Thus if the value of H_0 is confirmed, then either our theories of stellar evolution are wrong, or the standard model will have to be changed (some ideas that may be applied include:a period of double inflation, a lower density of the Universe, which would all but rule out the need for non-baryonic dark matter, or reintroducing Einstein's idea of a cosmological constant).

Many complementary projects are currently being carried out from the ground with the goal of providing values for the Hubble constant. However, they are subject to many uncertainties which HST was designed and built to circumvent. For example, a team of

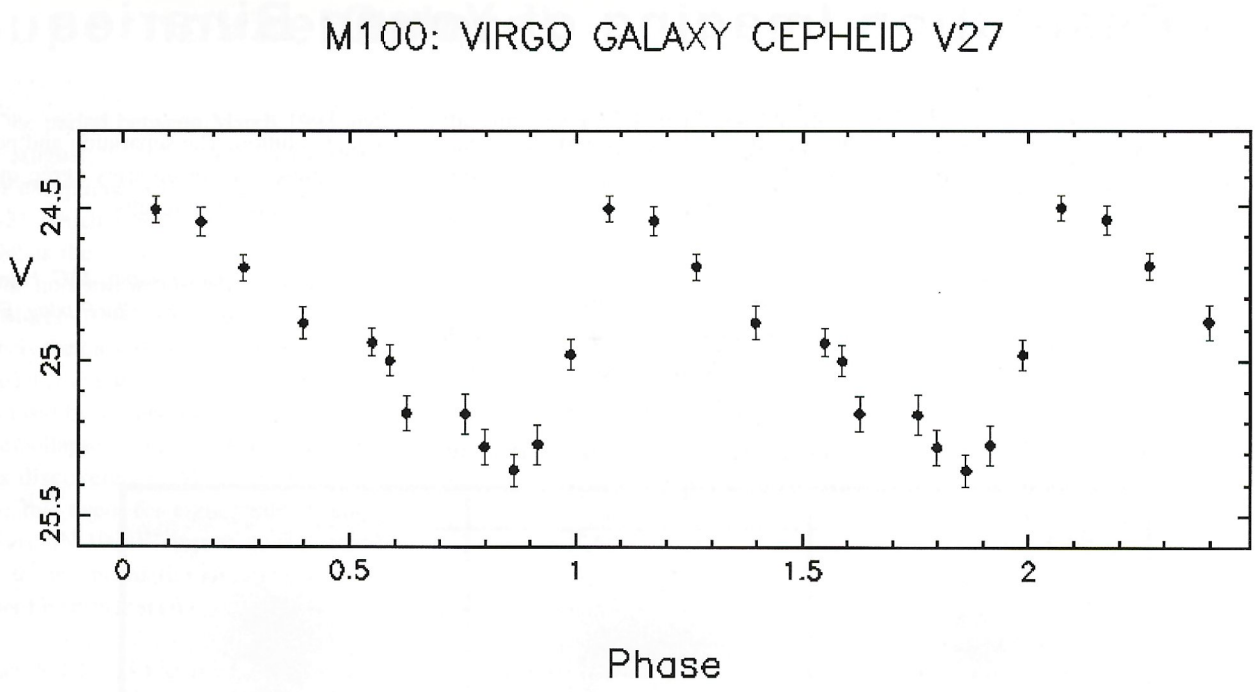

Fig. 2 – Light curve of the Cepheid variable shown in figure 1.

astronomers led by Michael Pierce (Indiana University) using the Canada-France-Hawaii telescope at Mauna Kea have recently arrived at a distance to another galaxy in Virgo (NGC4571 – see the September 29 issue of *Nature*) that is similar to that found for M100 using HST – but their result is tentative since it is based on only three Cepheids in crowded star fields. Another team led by Tom Shanks (University of Durham) and using the Martini adaptive optics system on the WHT had limited success in detecting variable stars in another Virgo galaxy IC3583 (see the last issue of *Gemini* No 42), but none of these were thought to be Cepheids.

Cepheid variables

The 20 Cepheids in M100 were identified from a series of HST Wide-Field and Planetary Camera (WFPC2) images, strategically placed in a two-month observing window. About 40 000 stars were measured in the search for these rare, but bright, variables. The distance was determined by comparing the Period-Luminosity relation to that obtained for Cepheids in the nearby Large Magellanic Cloud.

The Cepheid variables take their name from the star δ Cephei, which was discovered to be a variable in 1784 by the genius, deaf-mute astronomer John Goodricke from York. Cepheid variable stars are pulsating stars which regularly change in brightness with typical periods ranging from 5 – 70 days. For more than half a century, from the early work of the renowned astronomers Edwin Hubble, Henrietta Leavitt, Allan Sandage, and Walter Baade, it has been known that there is a direct link between a Cepheid's pulsation rate and its intrinsic brightness. However, it has only been since the refurbishment of HST and the advent of adaptive optics systems on ground-based telescopes that Cepheids have been detected in galaxies sufficiently distant that they are truly sampling the Hubble flow.

As a cross-check on the HST results, the distance to M100 has been estimated using the Tully-Fisher relation (a means of estimating distances to spiral galaxies using the maximum rate of rotation to predict the intrinsic brightness) and this independent measurement also agrees with both the Cepheid and Type II supernova (exploding massive young stars) 'yardsticks'.

Team members

The Key Project Team on the extra-galactic distance scale consists of Sandra Faber, Garth Illingworth and Dan Kelson (University of California, Santa Cruz), Laura Ferrarese and Holland Ford (Space Telescope Science Institute), Wendy Freedman, John Graham and Robert Hill (Carnegie Institution of Washington), James Gunn (Princeton University), John Hoessel and Mingsheng Han (University of Wisconsin), John Huchra (Harvard-Smithsonian Center for Astrophysics), Shaun Hughes (Royal Greenwich Observatory), Robert Kennicutt, Paul Harding, Anne Turner and Fabio Bresolin (University of Arizona), Barry Madore and Nancy Silbermann (JPL, Caltech), Jeremy Mould (Mt. Stromlo, Australian National University), Abhijit Saha (Space Telescope Science Institute), and Peter Stetson (Dominion Astrophysical Observatory, NRC).

Shaun Hughes, RGO

High Resolution Imaging of Young Binaries

The investigation of the occurrence and frequency of binaries among the youngest obscured stars has become a hot topic over the last few years. The highest spatial resolution studies usually rely on speckle imaging (Ghez *et al* 1993, *Astronomical Journal* **106**, 2005) and have found a very high incidence of binarity among young stars.

In recent tests of the common user real-time shift-and-add mode of IRCAM3, we have been able to resolve binaries with a resolution approaching that of speckle imaging. A sample of six images of sources from the list of Ghez et al are shown in figure 1, taken with UKIRT/IRCAM. Images were further processed using maximum entropy deconvolution. The separation and position angles of the binaries agree quite well with the Ghez results.

Colin Aspin, JAC, Hawaii,
Phil Puxley, ROE

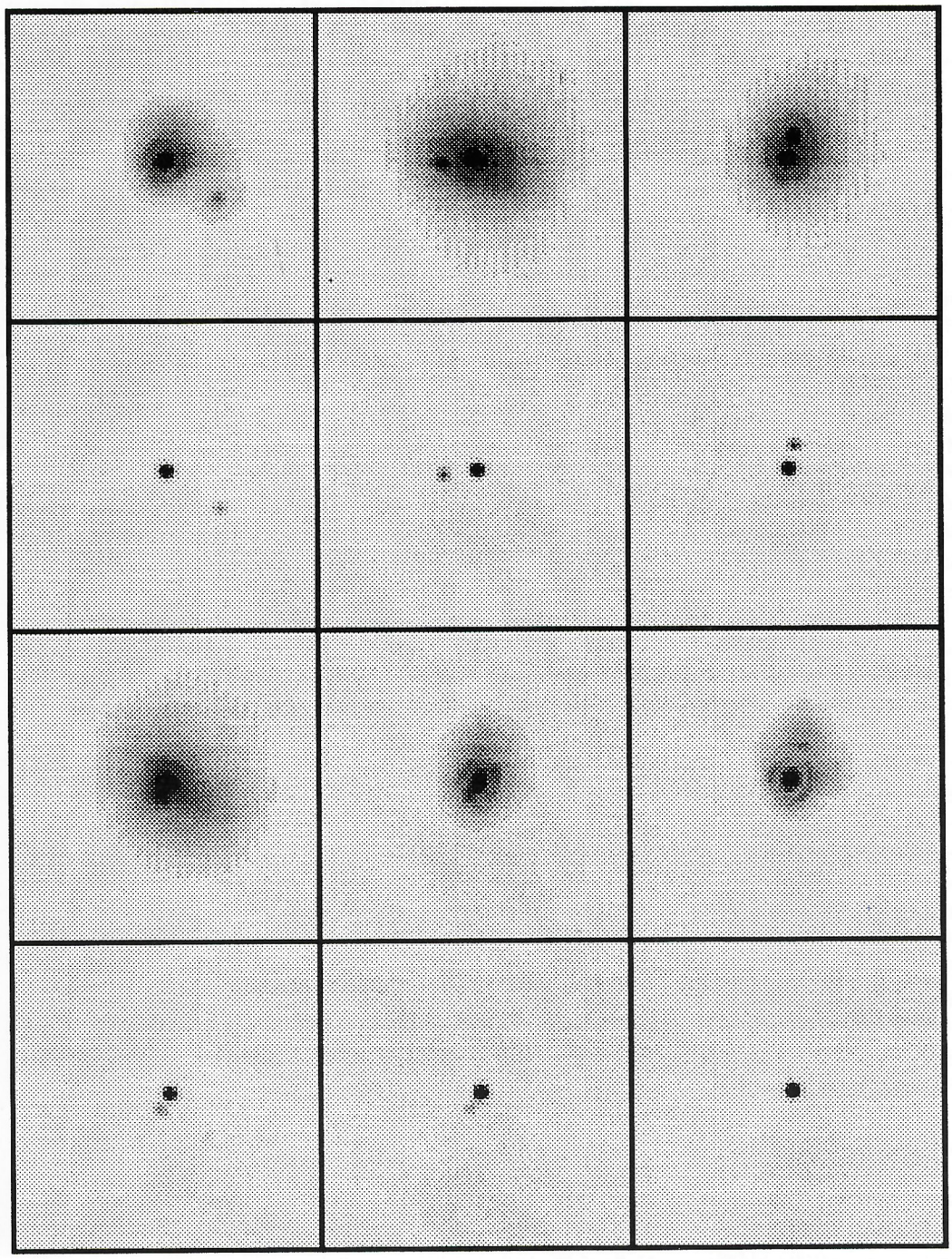

Fig. 1 – Images of six binaries from the list of Ghez et al. Images after processing with MEM are shown directly below each SAA image. From top left the sources and their binary separations are IRAS155203–2338 (0.8 arcseconds), V853 Oph (0.40 arcseconds), IRAS155913–2233 (0.29 arcseconds), IRAS160946–1851 (0.21 arcseconds), ROXS42c (0.16 arcseconds) and RNO90 (single).

Supernovae Galore!

The period between March 1993 and August 1994 saw the discovery of four exceptional supernovae. Supernova 1993J, which appeared in M81 in March 1993, is the closest core-collapse event in the northern hemisphere this century. In March 1994, SN 1994D exploded. This is the closest normal thermonuclear (type Ia) event for 22 years. This was followed by yet another two exceptional core-collapse events. In April SN 1994I was discovered in M51, the brightest type Ib/c event for eight years. Finally, in July SN 1994W appeared, and turned out to be one of the strangest type II supernovae ever seen.

When SN 1993J appeared, it was decided that the Isaac Newton Group (ING) telescopes would be used to obtain comprehensive coverage of this exceptional event. The data were quickly reduced at RGO and placed in an on-line computer archive. This proved to be very popular with the supernova community, and already over 10 publications based on the SN 1993J data archive have appeared, with more in the pipeline. The archive has now been extended to include the other three supernovae mentioned above. About 20 supernova astronomers, at 15 sites worldwide, are regularly accessing this very useful database. The archive can be accessed by anonymous ftp (131.111.68.35) in the directory **sn_archive** and subsequent subdirectories (see also *Spectrum* No 2, page 8). Users are requested to include the acknowledgement given in **acknowledgement.doc**, in any publications which make use of the archive.

Supernova 1993J in M81 (NGC 3031)

Spectroscopically, this was a type IIb event which means it was a bit like a type II at first *ie* it exhibited prominent H-lines, but as time went on the H I disappeared, with He I and heavier elements becoming prominent, as in a type Ib supernova. The consensus is that this was a core-collapse event in a progenitor which had lost nearly all of its hydrogen envelope as a result of interaction with a close companion. Much of the material, perhaps as much as 10 solar masses, may have formed a massive circumstellar cloud within which the supernova exploded. (See Meikle *et al*, *Gemini*, No 40, page 1, and Lewis *et al*, *Monthly Notices*, **266**, L27, 1994 for details about the early evolution.)

Four notable supernovae discovered over a 16 month period have been comprehensively monitored with the ING, CAMC and UKIRT telescopes.

Regular spectroscopic and photometric coverage of SN 1993J continues at the ING. Figure 1 shows the *UBVRI* light curves to 10 June 1994. Following its early second peak, the flux then declined monotonically. The rate of decline in all bands has been decreasing. At the time of writing (October 1994), the supernova is only about 2 magnitudes brighter than the progenitor was. Figure 2 shows the late-time spectral evolution. For much of 1993 the supernova spectrum was similar to that of a type Ib event – strong lines of oxygen, magnesium and calcium. However, during 1994, as most of the spectral lines faded, a wide, square-shaped profile appeared, blended with the red edge of the [OI]6300,64 Å feature. In figure 3, the region around the square profile is shown. It can be seen that, as the supernova faded, the square profile flux remained roughly constant. By day 530 (8 September 1994) the [OI] had mostly vanished leaving the square profile centred on 6549 Å. The position of this feature strongly suggests Hα emission, blueshifted by about 500 km/s with respect to the rest wavelength in the supernova centre of mass frame. The width corresponds to an expansion velocity of 10 000 km/s.

A wide square profile results if the emitting zone is a thin, rapidly expanding

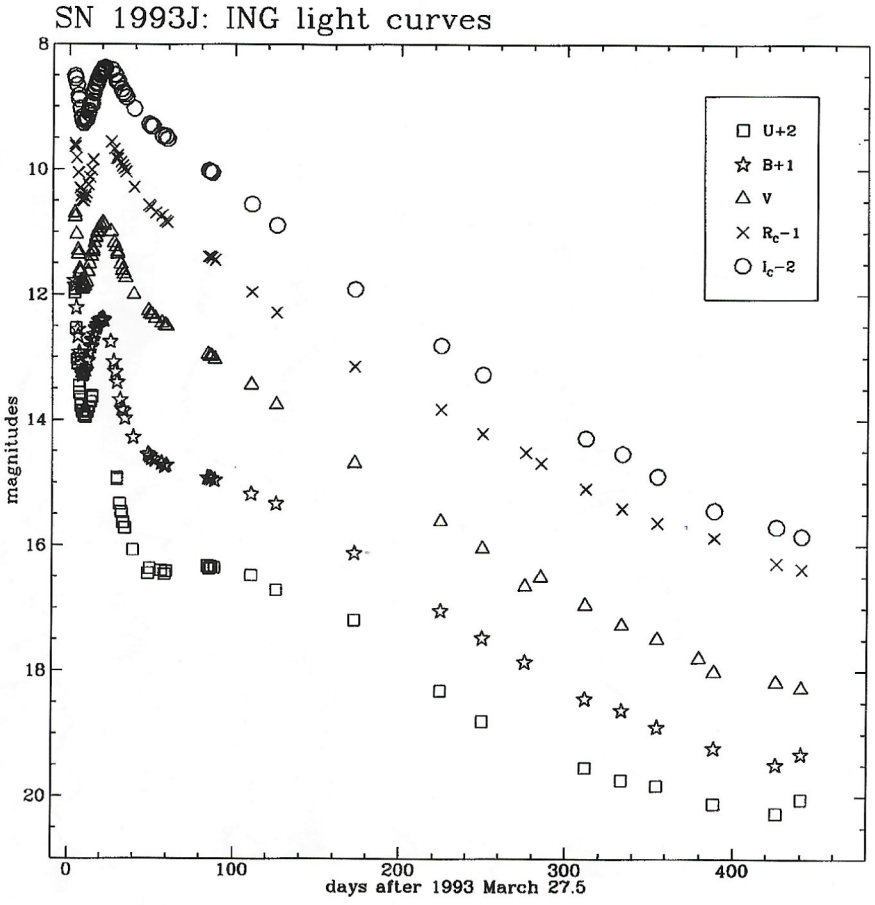

Fig. 1 – UBVRI light curves of the type IIb Supernova 1993J, obtained using the Isaac Newton Group telescopes. For clarity they have been displaced vertically by the amounts shown in the box. The x-axis gives the number of days after the estimated explosion date on 27.5 March, 1993.

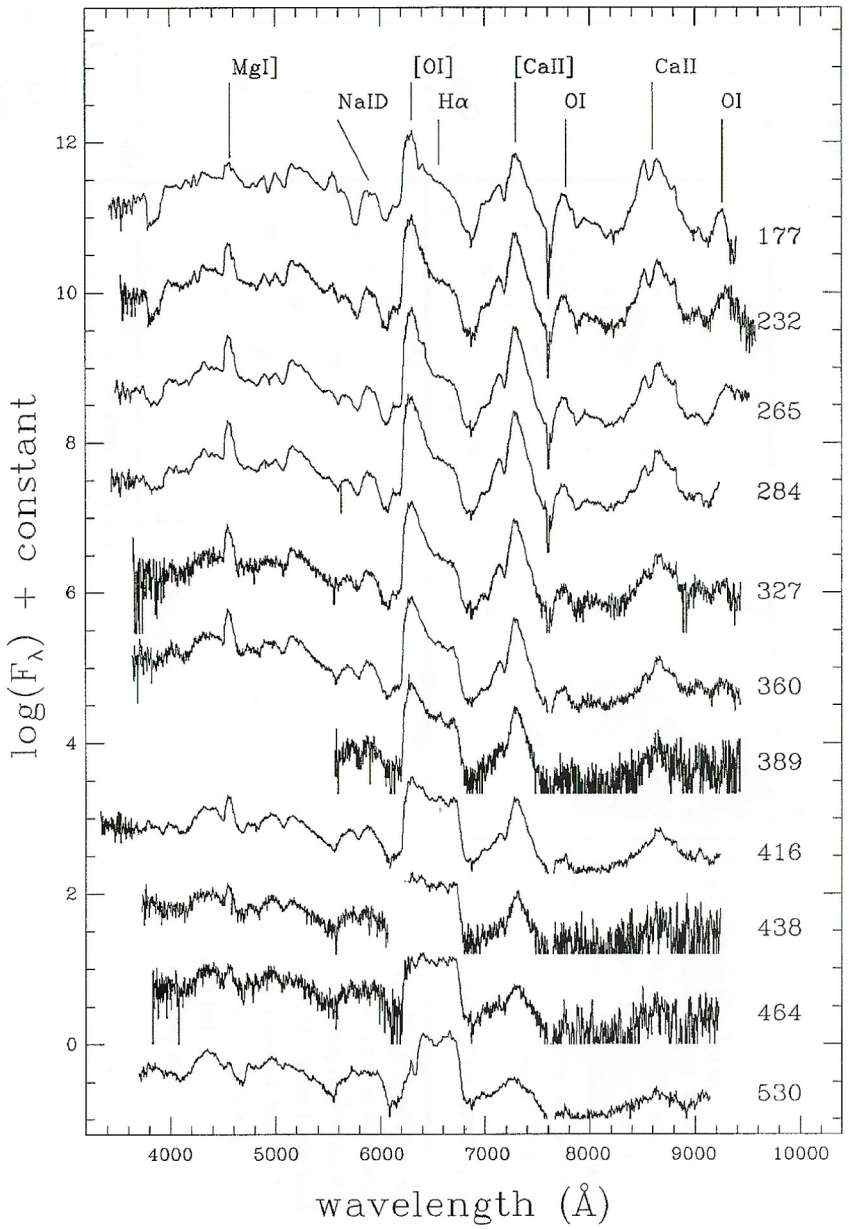

Fig. 2 – Late-time optical spectra of the type IIb Supernova 1993J obtained at the INT and WHT. The data are plotted on a logarithmic flux scale, and displaced vertically for clarity. The numbers on the right hand side give the days after explosion. Day 530 is 8 September 1994. Between days 177 and 530, the flux declined by a factor of about 40.

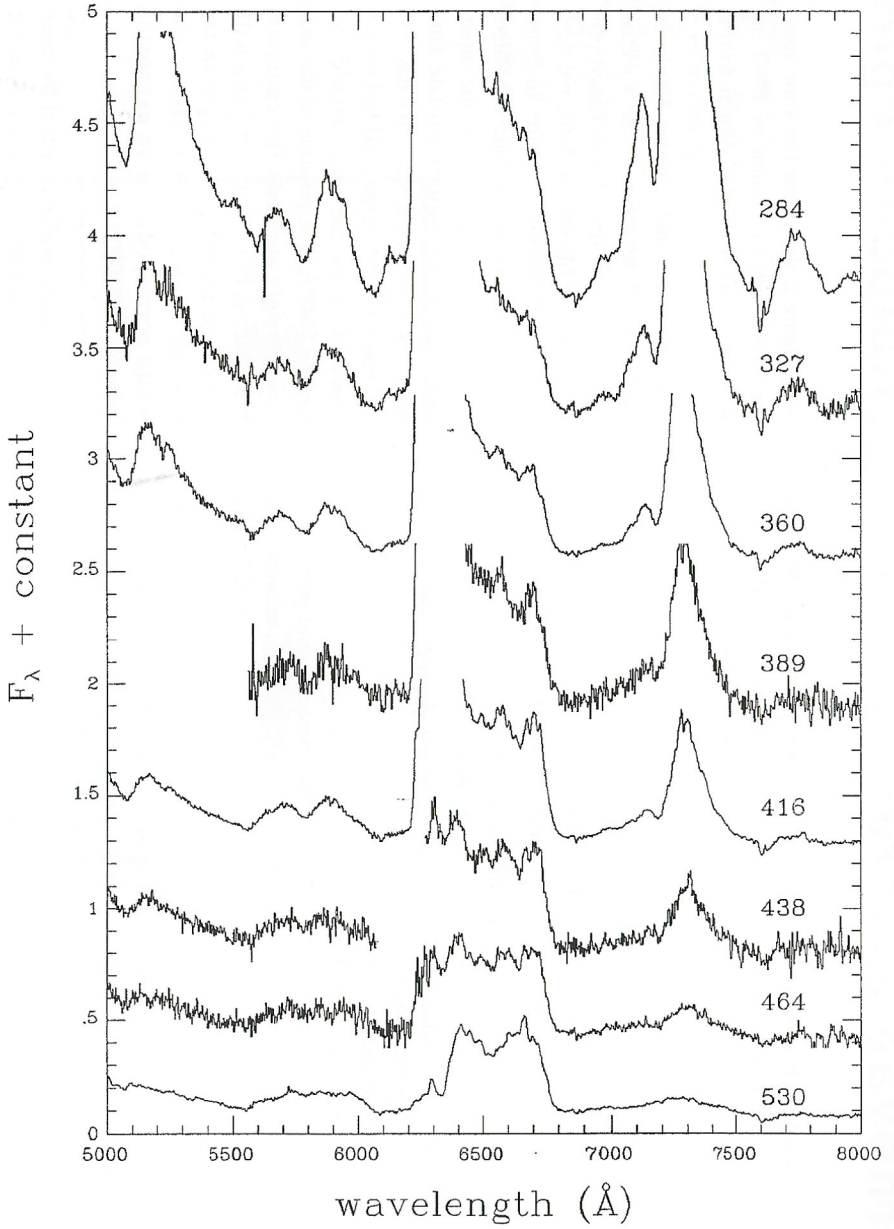

Fig. 3 – Close-up of the late-time optical spectra of Supernova 1993J. The spectra are all plotted on the same linear flux scale, and have only been displaced vertically for clarity. The numbers on the right hand side give the days after explosion.

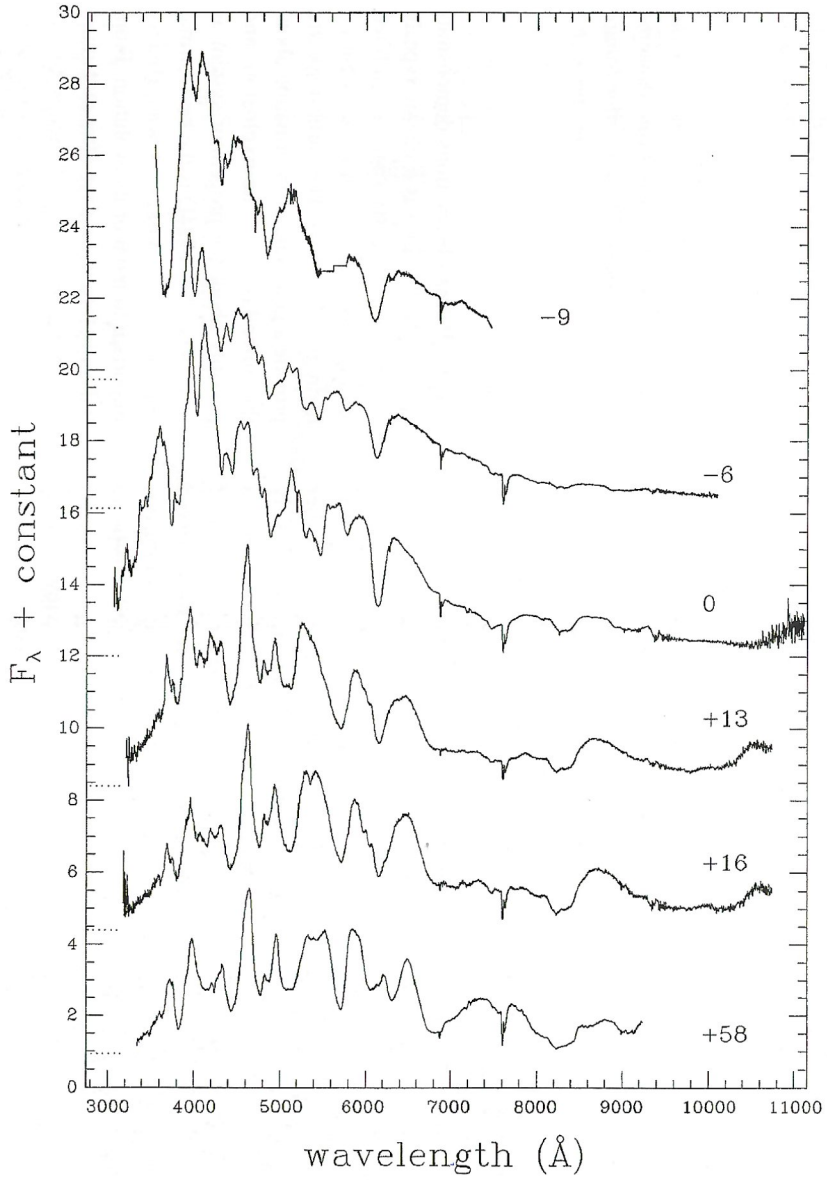

Fig. 4 – Optical spectra of the classic type Ia Supernova 1994D acquired at the INT and WHT. The numbers on the right hand side give the epoch in days relative to maximum blue light on March 21.0. The spectra have been displaced vertically for clarity. The dotted lines on the left hand side give the zero flux for each spectrum. The spectra for days –6 to +16 are on the same relative flux scale. The spectra for days –9 and 58 have been arbitrarily scaled. Most of the lines in the early spectra are due to Mg II, Si II, S II, and Ca II, while the later spectrum (day 58) exhibits iron emission.

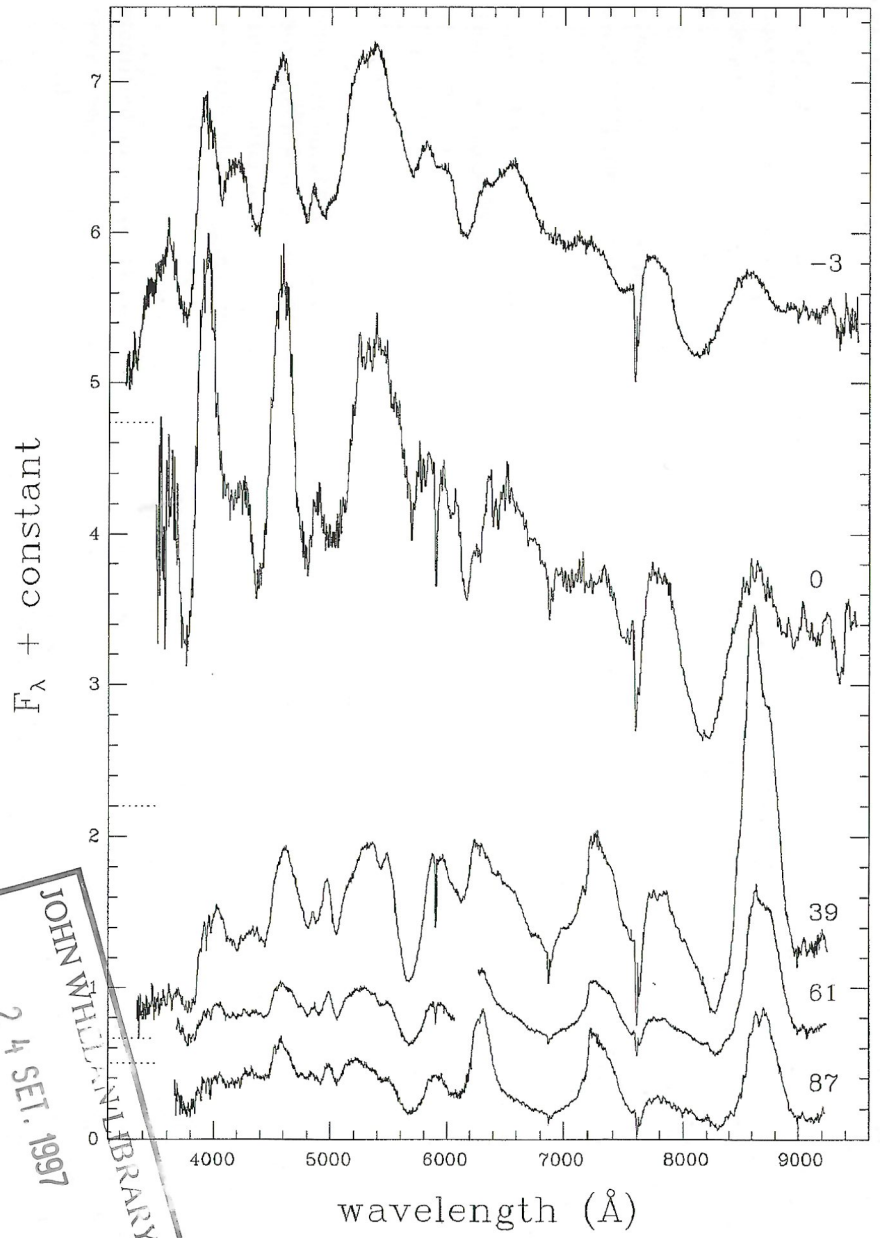

Fig. 5 – Optical spectra of the type Ic Supernova 1994I obtained at the INT and WHT. The numbers on the RHS give the epoch in days relative to maximum blue light on April 8.0. The spectra have been displaced vertically for clarity. The dotted lines on the LHS gives the zero flux for each spectrum. The fluxes of the first two spectra have been multiplied by a factor of 0.1, relative to the other three spectra.

shell of material. The slight dip in the middle implies a departure from radial symmetry; *eg* the shell may be somewhat flattened. The constancy of the flux suggests the presence of a power source in addition to the decay of radioactive cobalt in the ejecta. The luminosity (assuming symmetrical emission, and correcting for extinction) is around 4×10^{38} ergs. This large luminosity rules out long lived isotopes (*eg* ^{44}Ti as the power source – too much would be required. Pulsar emission also seems unlikely since this would tend to preferentially affect slow moving material near the centre *ie* it cannot explain the huge observed velocities. The most likely explanation is that we are seeing the impact of the ejecta onto the massive progenitor wind. Indeed, given the strong observational and theoretical evidence for a huge mass loss from the progenitor, the appearance of the square Hα profile is perhaps not very surprising.

As the ejecta run into the circumstellar medium (CSM), line emission is produced in two regions. When the supernova shock heads into the CSM, a reverse shock travels inwards through the supernova ejecta. Both shocks produce X-rays: the observed line probably originates from X-ray-ionised supernova ejecta, both just inside and just outside the reverse shock. The steep density gradient in the ejecta (required to account for the supernova's light curve) ensures that the minimum velocity seen in the shell remains approximately constant in time, at around 10 000 km/s. The impact of ejecta on previously-lost progenitor material has been observed in other supernovae (SN 1970G, 1979C, 1980K). However, SN 1993J has provided us with the fastest, most powerful example of this phenomenon that has ever been seen. Continued observation of this supernova is vital. As the reverse shock ploughs deeper into the ejecta, it can provide a tool with which to examine the abundance distribution and hence probe the physics of the actual explosion.

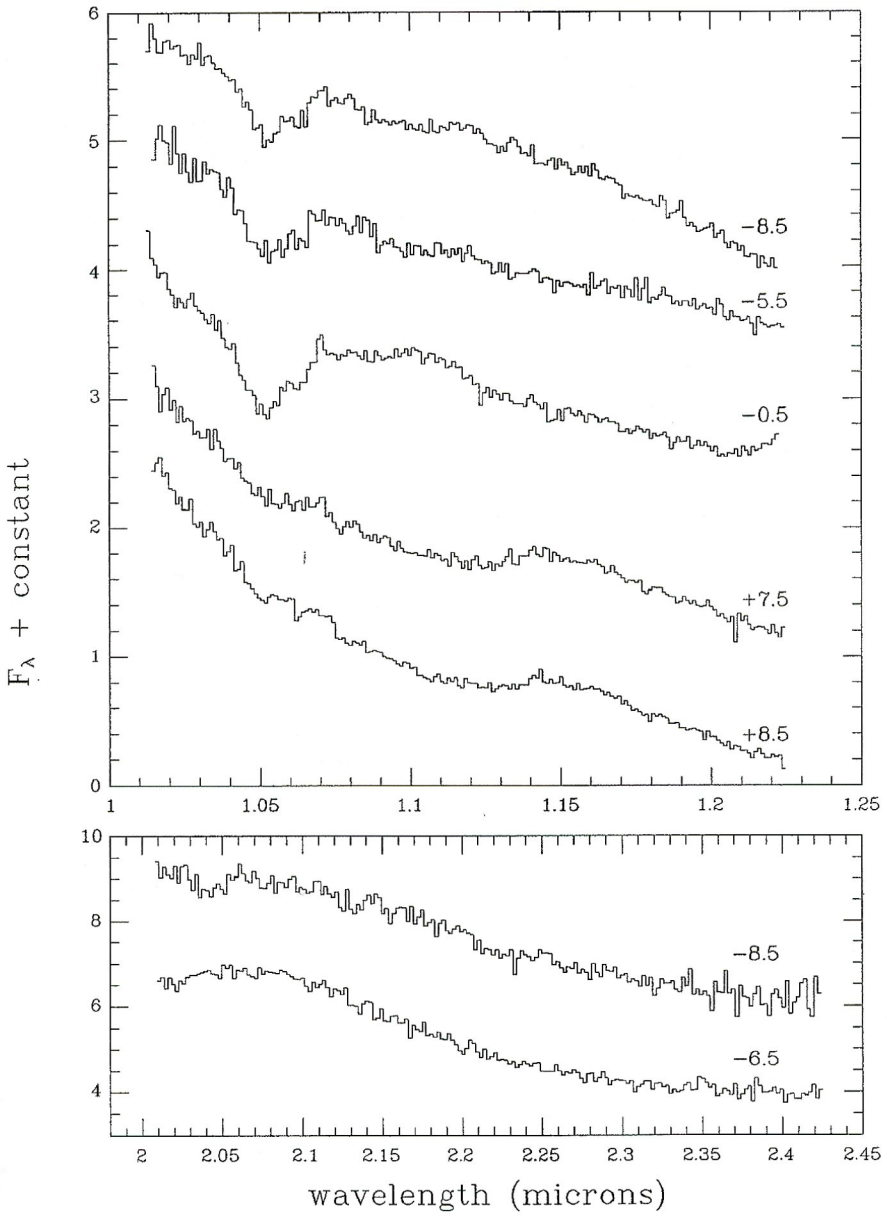

Fig. 6 – J- and K-band spectra of Supernova 1994D, obtained at UKIRT. The numbers on the right give the epoch in days relative to maximum blue light on March 21.0. This figure shows the first ever high quality, pre-maximum IR spectra of a type Ia supernova. The absorption feature at about 1.05 μm is attributed to He I, and is discussed in the text. The J-window spectra for days –5.5 to +8.5 are on the same linear flux scale, and have only been displaced vertically for clarity. The day –8.5 J-spectrum has been arbitrarily scaled.

Supernova 1994D in NGC 4526

Type Ia events are believed to arise from the thermonuclear fusion of carbon and oxygen in a white dwarf in a close binary system. Mass transfer from the companion triggers the explosion, probably by taking the white dwarf to the Chandrasekhar limit. However, neither the evolutionary history of the progenitor, nor the propagation of the explosion wave are well understood. The companion may be a non-degenerate helium star or it may be another white dwarf. The explosion is unlikely to be due to either a pure detonation or a pure deflagration wave since neither of these mechanisms produce the observed abundances at the correct velocities. Given that we believe most type Ia supernovae form a highly homogeneous class, and particularly in view of their use as cosmological distance indicators, it is clearly important to improve our understanding of these events.

The La Palma observations demonstrated that SN 1994D was a classic type Ia supernova *ie* its early spectra exhibited strong silicon absorption features but no hydrogen (figure 4). The earliest spectra provide a goldmine of information about the outer layers of the explosion, and possibly about the progenitor system as well. Since SN 1994D is the best normal type Ia for 22 years, it was clearly important to monitor its evolution. From 9 days before to 16 days after maximum blue light, regular spectroscopy by the ING telescopes, together with photometry by the ING and the Carlsberg Automatic Meridian Circle (CAMC),

was carried out. This work has placed SN 1994D among the mere handful of type Ia supernovae which have such complete pre/post maximum optical coverage. Most of the lines in the early spectra are due to Si II, S II, Mg II and Ca II, while the later spectrum (day 58) exhibits iron emission. The CAMC also obtained an astrometric position of this event (IAU Circular 5976).

As well as the ING and CAMC telescopes, the United Kingdom Infrared Telescope (UKIRT) participated in the early observations, providing the first ever high quality, pre-maximum infrared spectra of a type Ia supernova (figure 6). *J*-window spectra taken before maximum light exhibited a broad absorption feature around 1.05 μm. This vanished after maximum light. The most likely identification of this feature is a P Cygni profile in He I 1.083 μm. Helium has never before been clearly identified in a type Ia supernova. Indeed, because of this, it is not even included in many explosion models. If the helium identification is correct, then we might also expect He I features at 5876 Å and 2.058 μm. The *K*-window spectra are inconclusive as the large blue shift of the line would have pushed the greater part of any He I absorption to beyond the blue limit. However, there is a feature at about 5760 Å in contemporary ING optical spectra. In previous supernovae, this feature has been attributed to the P Cygni absorption component of Si II 5972 Å, but possibly part of this feature is due to He I 5876 Å.

The lower level of the He I 1.083 μm transition is the high excitation, but highly metastable, $2s^3S$ level. Simple He I P Cygni modelling of the features at 1.05 μm and 5760 Å suggests a population of about 0.3 cm^{-3} in the $2s^3S$ level. It is not immediately clear how this is populated, but simple LTE collisional excitation seems a possible explanation. The level of the continuum in contemporary ING spectra indicate a temperature of around 13 000K. This could produce the $2s^3S$ population deduced from the P Cygni lines from a total He I mass of 6×10^{-5} solar masses. However, the deduced mass is very sensitive to temperature – for 10 000K, a mass as large as 0.01 solar masses would be inferred. This high sensitivity to temperature would explain why the He I 1.083 μm line disappeared soon after maximum light, due to the cooling of the ejecta. If the helium mass is indeed as high as 0.01 solar masses, it may favour a helium star for the progenitor companion. A paper describing this work is in preparation.

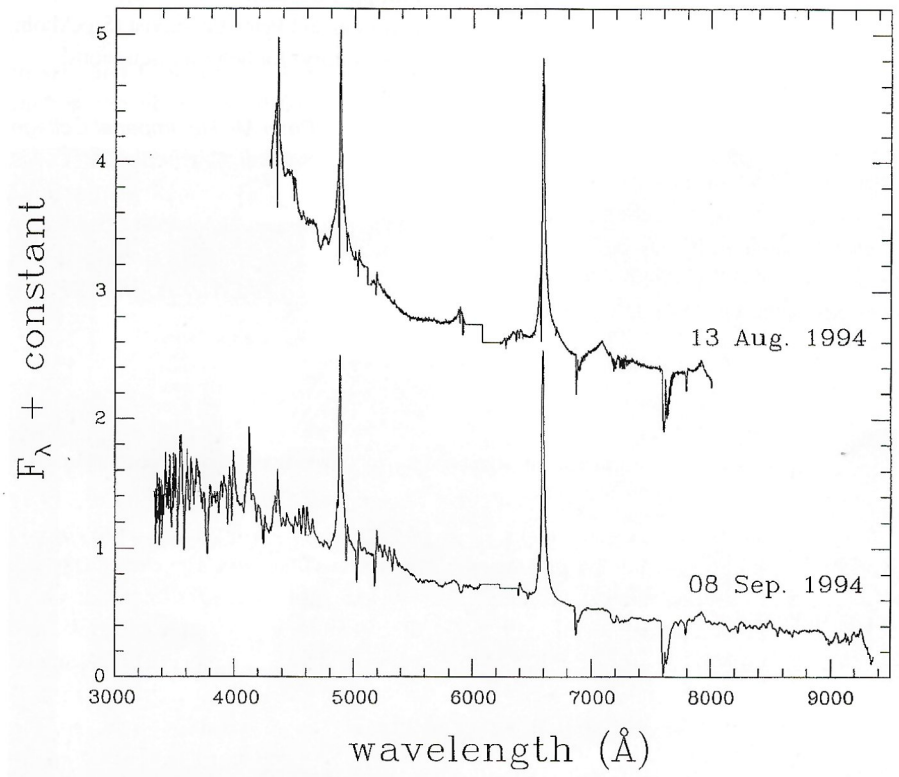

Fig. 7 – Optical spectra of the peculiar type II Supernova 1994W obtained at the WHT. The August 13 spectrum has been displaced vertically for clarity, and has twice the resolution of the September 8 spectrum. Many narrow P Cygni profiles can be seen. These include Hα, Hβ, Hγ, He I 5876, 6678 Å, O I 7773 Å, Mg II 4481 Å, Si II 6347, 6371 Å, Fe II 4549, 4583, 4629, 4923, 5018, 5169 Å.

Supernova 1994I in M51 (NGC 5194)

Type Ic supernovae are another fairly recent addition to the menagerie of core-collapse supernovae. They are characterised by a lack of, or weak, hydrogen lines, and they do not exhibit the strong helium lines found in type Ib. They also have a relatively fast declining light curve. ING observations began three days after the discovery, and the spectra (figure 5) confirm that SN 1994I was a type Ic event. An astrometric optical position and *V* light curve were obtained using the CAMC (IAU Circular 5989).

The exact origin of the Ic sub-type is still controversial. Nomoto *et al* (*Nature*, **371**, 227, 1994) have recently suggested a progenitor in a close binary system, where not only does the progenitor lose its H-rich envelope, but also its helium envelope, becoming a bare C+O star of mass ~2 solar masses before collapse. They suggest different scenarios leading to this result. To improve our understanding of these events, good spectral coverage plus detailed spectral modelling is required to derive densities and abundances. It is hoped to continue monitoring this event well into 1995.

Supernova 1994W in NGC 4041

ING spectra of this very peculiar type II event taken about 3 and 6 weeks after the explosion are shown in figure 7. The spectra are dominated by strong Balmer emission lines. These have a width at half maximum equivalent to 1000 km/s, which is unusually slow, superimposed on a much wider base. Narrow absorption lines are also present, blueshifted by 600 km/s with respect to the line peaks, and with widths of only about 300 km/s (see figure 8). Narrow P Cygni features in He I, O I, Mg II, Si II and Fe II can also be seen in figure 7, as well as broad emission in the He I lines. Few other supernovae with this type of spectrum have been seen.

The spectra appear to be arising from two different origins. The broad hydrogen and helium emission arise from the rapidly-moving ejecta, while the narrow

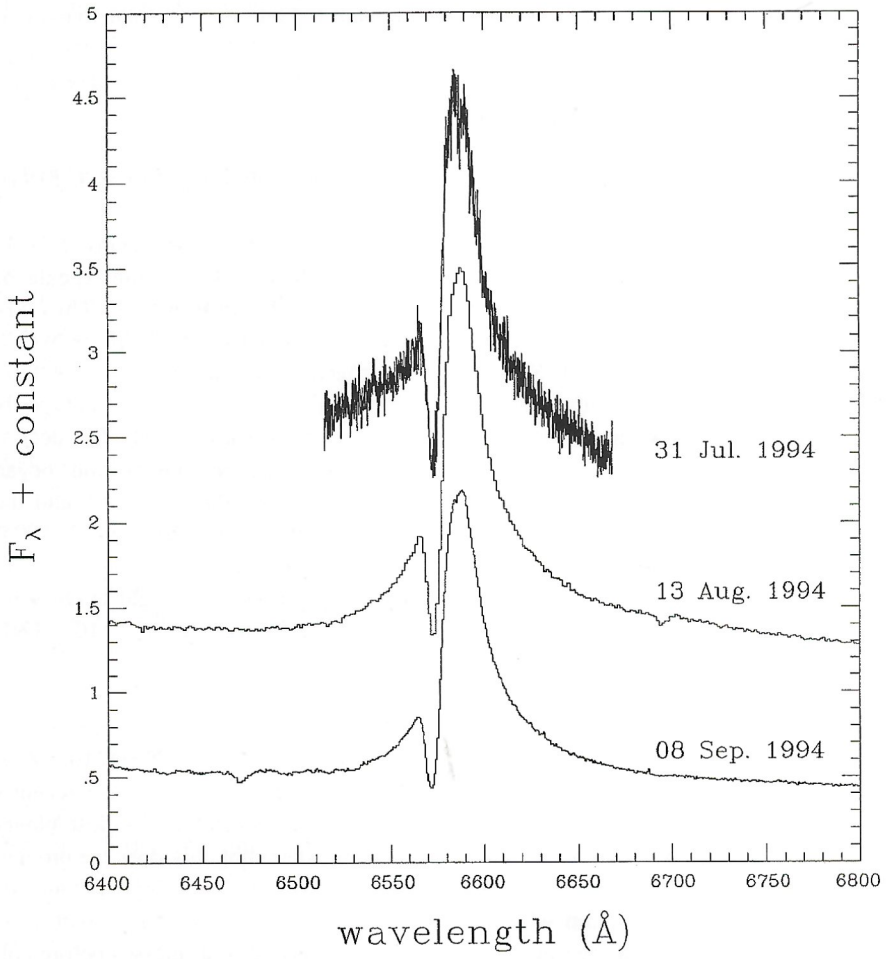

Fig. 8 – Detail of the optical spectra of Supernova 1994W, illustrating the Hα feature at three epochs. The August and September spectra are on the same relative flux scale, while the July spectrum has been arbitrarily scaled. The spectra have been displaced vertically for clarity. Note that the September 8 spectrum shown here is at four times the resolution of the spectrum shown in figure 7.

P Cygni lines are probably due to a slow-moving, dense circumstellar wind released by the progenitor, which was ionised by the supernova EUV flash, and is now scattering part of the subsequently emitted optical light. The spectrum taken on 8 September shows that, while the broad emission lines had weakened somewhat, the equivalent widths of the metal lines had all increased. The distribution of the circumstellar material is presently unclear. It may be in the form of a distinct shell. If this is the case then we expect the ejecta to collide violently with the shell very soon, becoming a strong X-ray and radio source. Observations are continuing.

Conclusion

The discovery of four notable supernovae over a 16 month period is unusual but, nevertheless, is probably just a random fluctuation in the observed rate. More important is the fact that all three of the core-collapse events were peculiar. It is gradually becoming clear that core-collapse supernovae produce a continuum of observational sub-types. For at least two of the three core-collapse events (93J and 94I), it is possible that a companion played an important role. The diversity of core-collapse subtypes may be due, at least partly, to differences in binary history. Thus, binary progenitors are likely to be important for core-collapse supernovae as well as for thermonuclear events.

Acknowledgements

This project involves a large number of people. We especially thank the very many guest and staff astronomers who carried out the supernova observations at CAMC, ING and UKIRT. We also thank Philipp Podsiadlowski (IoA), and Claes Fransson and Peter Lundqvist (Stockholm Observatory) for helpful discussions.

Peter Meikle, Imperial College,
Robin Catchpole, Jim Lewis,
Ralph Martin, RGO,
Robert Cumming, Stockholm Observatory,
Tom Geballe, JACH,
Nic Walton, ING La Palma

RGO Preprints

204
R G M Rutten and V S Dhillon
Roche tomography: imaging the stars in interacting binaries.
Astronomy and Astrophysics, Main Journal

205
M D Still, V S Dhillon and D H P Jones
Emission line variations of the nova-like variable PX Andromedae (=PG0027+260).
MNRAS

206
J V Wall
Populations of extragalactic radio sources.
Contributed paper at John G Bolton Memorial Symposium

207
R J Terlevich, G Tenorio-Tagle, M Rozyczka, J Franco and J Melnick
The starburst model for active galactic nuclei II, the nature of the lag.
MNRAS

208
C R Benn and J V Wall
Structure on the largest scales – constraints from radio-source-count isotropy.
MNRAS

209
B J Boyle, T Shanks, I Georgantopoulos, G C Stewart and R E Griffiths
A deep *ROSAT* survey – IV. The evolution of X-ray-selected QSOs.
MNRAS

210
B J Boyle, R G McMahon, B J Wilkes and M Elvis
The Cambridge-Cambridge ROSAT Serendipity survey – I. X-ray-luminous galaxies.
MNRAS

211
M D Still, V S Dhillon and D H P Jones
Spectrophotometry of the nova-like variable RW Trianguli in a high state.
MNRAS

212
K Lipman and M Pettini
Interstellar titanium in the Galactic halo.
Astrophysical Journal

SuperCOSMOS Comes into Operation

SuperCOSMOS is the latest addition to the UK Wide-Field Astronomy programme. Housed at the Royal Observatory Edinburgh (ROE), the facility is nearing completion and is being thoroughly tested before coming into routine operation from 1 January 1995. SuperCOSMOS is 10 times more powerful than its predecessor, COSMOS, and will provide a new, very high-speed, high-precision tool for the UK community.

The heart of the machine (figure 1) consists of a granite air-bearing *xy* table providing high accuracy position measurements, a linear CCD array (of 2048 pixels) for the high-speed scanning capability and transputers and DEC Alpha workstations for rapid data processing. The entire system is housed in an environmental chamber, providing class 100 clean-room conditions and high thermal stability (temperature maintained to ±0.05°C over a 24 hour period) thereby ensuring strict integrity of the data during the scan process. The system is also isolated against external vibrations.

Glass plates up to 20 × 20 square inches in size and films up to 14 × 14 square inches can be accepted for scanning. The photographic material is digitised to 15 bits with a resolution of 10μm. The dynamic range is greater than 3 densities (diffuse) above sky background. The central 320 × 320 mm^2 area of a Schmidt plate is digitised in a timescale of two hours, producing some 2 Gbytes of pixel data.

SuperCOSMOS, ROE's new high-speed, high precision measuring machine, comes into routine operation on 1 January.

These data are currently processed using the COSMOS crowded-field analysis software producing a catalogue of all the objects detected above the detection threshold, with some 32 parameters stored for each image (IAM data). Ultimately, it is our aim to develop more sophisticated algorithms for a more complete exploitation of the information content from astronomical plates.

As well as the final IAM parameters for the objects detected, users can receive the full pixel data for their plates. This has been of immense value for projects involving digital coaddition of the pixel data from several plates of the same field. In field 287, for example, where Hawkins has large numbers of plates, experiments with COSMOS have indicated that on the master plate in the series objects at $B=22^m$ are just detectable, while after stacking 66 J plates objects down to at least $B=26^m$ can be seen, and this for the entire field of the scanned area (36 square degrees). The use of SuperCOSMOS with digital coaddition techniques provides a powerful way of obtaining very deep wide-angle samples, and opens up new potential for the Schmidt Telescope-measuring machine combination.

In addition to the routine scanning of users' plates on request, a prime background task on the facility will be the systematic digitisation of the photographic material from the major sky surveys (UKST and ESO in the South, POSS in the North). The raw pixel data from these surveys will be routinely archived and will be made generally available through time. However, initially the main goal will be to produce a highly accurate multi-colour, multi-epoch Object Catalogue of both Southern and Northern skies. This will provide a powerful tool for both direct astronomical research based on the catalogue as well as fundamental support for telescope and satellite observations.

Harvey MacGillivray, Bill Cormack, Lance Miller, ROE

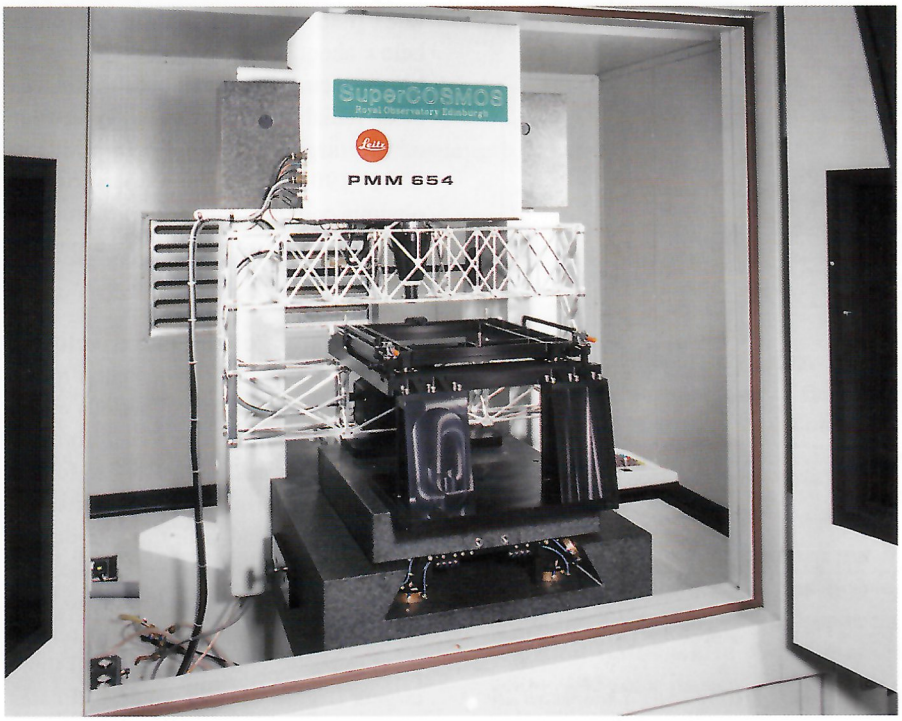

B W Hadley

Fig. 1 – SuperCOSMOS, seen here within its environmental chamber. Also seen are the xy table, the holder within which the plate is situated and the scanner/detector assembly.

Fossils of the Common Envelope Phase

When most stars retire from active life, they become white dwarfs. Since the maximum mass of a white dwarf is around 1.4 solar masses they must shed a great deal of mass in the process and understanding how they manage this is of considerable interest. The structure of white dwarfs is well enough understood for it to be possible to derive masses from their spectra alone. When this is done, one finds a mass distribution sharply peaked around 0.55 solar masses. This is a consequence of the ignition of helium which occurs at a core mass of 0.45 solar masses. The ignition of helium marks the end of the red giant branch and eventually leads to the asymptotic giant branch and the loss of most of the star's mass, which is reflected in the final mass of 0.55 solar masses.

White dwarfs can form with masses below 0.45 solar masses but only from stars of mass so low that they cannot have left the main-sequence in the lifetime of the Galaxy. Nevertheless, there are some low mass white dwarfs known, and in a recent study about 10% of the targets had masses below 0.45 solar masses. Low mass white dwarfs are a natural consequence of binary evolution for if a star ascending the red giant branch encounters its Roche lobe (which marks the maximum size set by tidal forces), it will rapidly lose its envelope to its companion and nuclear burning will cease.

The discovery of five new white dwarf binaries confirms that binary evolution has a significant impact on the white dwarf mass distribution.

For us to see the white dwarf now, its companion must itself be compact or of very low mass, and such stars cannot accrete mass at a high rate. Therefore during the stage of rapid mass transfer, an envelope forms common to both stars. This envelope is then ejected as energy is transferred from the orbit of the binary. The binary emerges in a much tighter orbit than it had at the start of mass transfer because a mass comparable to the mass of the remnant is ejected. Common envelope evolution can thus have a dramatic effect on a binary, shrinking the orbit by factors of 100 or more and even leading to a merger of the two stars.

Assuming that the stars avoid merging, we expect that low mass white dwarfs should be in binaries, and moreover, that they should be in close binaries. We undertook observations to test these predictions, and in a rare example of reality meeting expectation we found five binaries out of seven targets.

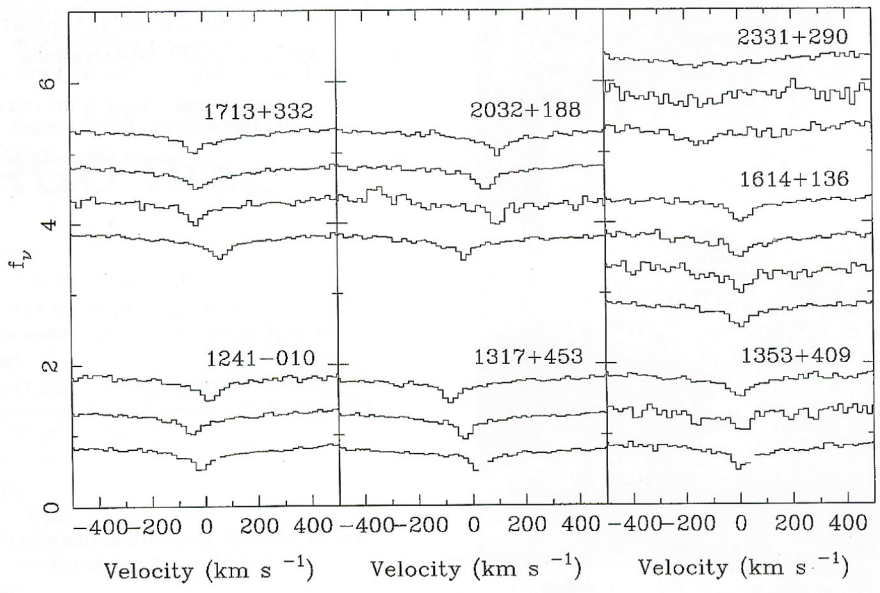

Fig. 1 – The spectra of the WHT targets within ±500 kms^{-1} of Hα (6562.76Å). The spectra are the average of the data from each night separately and are plotted such that time ascends. The broad wings of Hα extend far beyond the range plotted here.

Observations

Our first run was of three nights on the WHT and ISIS in June 1993. The nights were scheduled with gaps in between to increase our sensitivity to long orbital periods. The two most likely companions were other white dwarfs and very low mass main-sequence stars, and therefore we needed to look for radial velocity variations (for white dwarf companions) and for molecular bands (for low mass main-sequence companions). On the advice of Dr R Saffer, it appeared that Hα was the best line to use for radial velocity work as it often shows a sharp core caused by non-LTE effects. Luckily a dichroic was available that separated red and "blue" at a wavelength of 7500Å, allowing us to observe Hα on the blue arm and in the *I*-band on the red arm.

The red spectra showed no sign of any late-type features, and by adding in the spectrum of an M dwarf standard star, we estimate that any main-sequence companion must have a spectral type later than M6 (and therefore a mass below about 0.1 solar masses). Once the blue spectra were reduced, there was clear radial velocity variability in four of the targets (figure 1). In addition 2331+290, which does not show an obvious core in figure 1, varies on short time-scales, suggestive of a period around two hours.

Consideration of the radial velocity changes and probable companion masses led to estimated orbital periods of the order of a week or less. Therefore we applied for a week on the INT to follow three of the brightest WHT binaries. This was observed with the IDS during April 1994. Despite the loss of the first night from cloud, we were able to confirm our WHT detections and obtain good radial velocity curves for all three targets (figure 2). Our crude estimates of the periods worked out remarkably well – we find periods of 3.35, 4.87 and

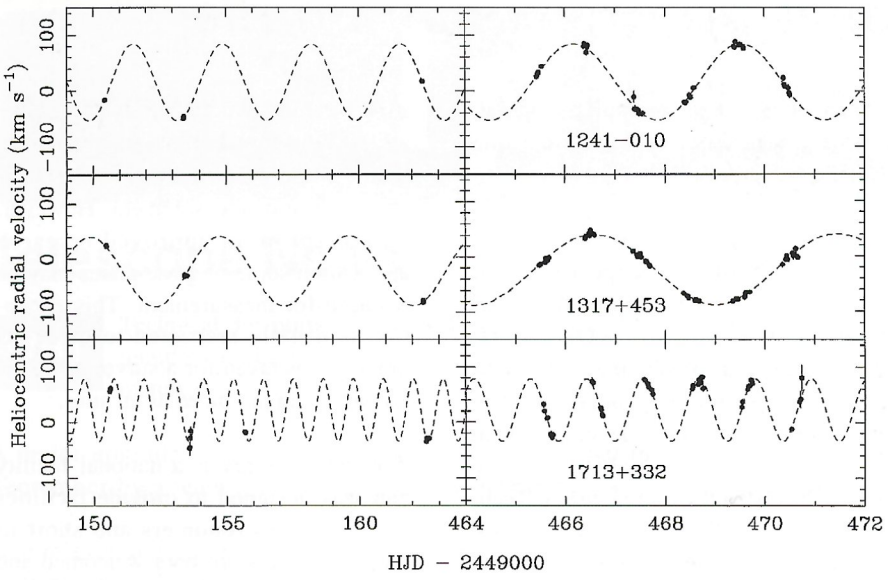

Fig. 2 – The radial velocities are displayed along with 1σ error bars and dashed lines showing best-fit circular orbits. The left panels show the WHT data and the right panels show the INT data. 1σ error bars are plotted, but are often smaller than the points.

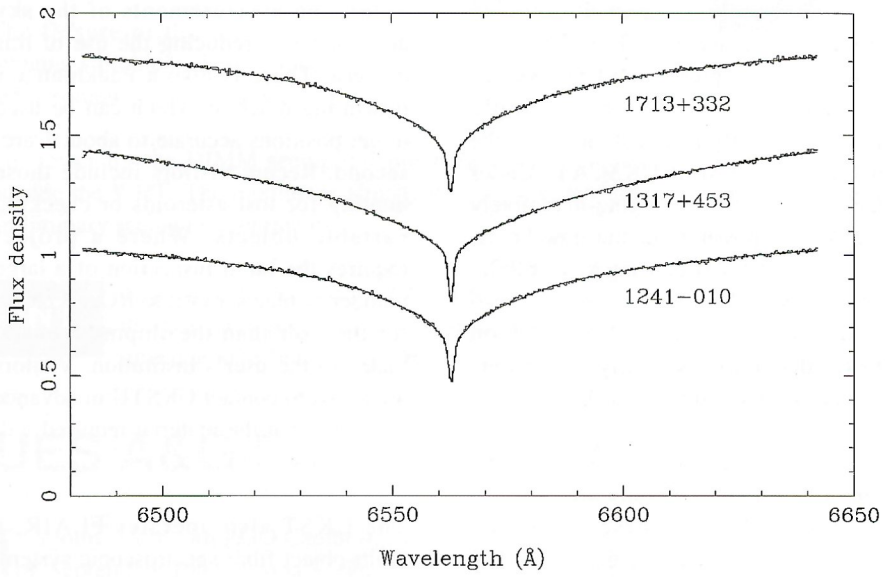

Fig. 3 – The mean INT spectra (with the radial velocity variations shifted out) are plotted with an offset of 0.4 units along with multiple gaussian fits which were used to obtain the velocities plotted in figure 2.

1.13 days for white dwarfs 1241−010, 1317+453 and 1713+332. Sparse sampling precludes accurate estimates for the other two binaries, but periodogram analysis suggests periods close to five or ten days (harmonically related periods) for 2032+188, and, as we mentioned above, a very short two hours for 2331+290 (based mainly on changes that occurred on the third night of the run). Figure 3 shows the average INT spectra plus fits of multiple gaussians that we used to measure the radial velocities. This shows nicely the advantage of Hα compared to other Balmer lines which do not possess the sharp central core.

Discussion

The discovery of five binaries out of seven targets confirms that binary evolution has a significant impact upon the distribution of white dwarf masses below 0.45 solar masses. From our INT data we can also determine the mass functions of three of the binaries, and in combination with our upper limit upon the mass of any main-sequence companion, we find that the companion stars must also be white dwarfs. To our knowledge only two other double degenerate binaries have been found from radial velocity studies which have looked at about 100 targets (about five others are known from atmospheric analysis, but it may never be possible to determine their orbital periods). Our high "hit-rate" is presumably a result of selecting low mass targets but also the use of Hα on a large aperture telescope which led to uncertainties in the radial velocities of order 3 km s^{-1}, much lower than in previous studies.

Gravitational radiation is the only known way in which pairs of well-separated white dwarfs can change their orbital periods. Gravitational radiation will force the binaries to merge in a time $-3P/8\dot{P}$ where P is the present orbital period and $\dot{P}$ is its rate of change. For our targets the spiral-in time is about $5 \times 10^7\ (P/1\,\mathrm{hr})^{8/3}$ years. For orbital periods much above about ten hours, the orbital periods are effectively frozen since the time-scale exceeds the age of the Galaxy. Even 2331+290, with an orbital period of about two hours, cannot have changed much since the common envelope phase, since its cooling time is 10^7 years, compared to $-P/\dot{P}$ of 10^9 years.

Our targets are therefore end-points of common envelope evolution. The next steps will be to build up an orbital period distribution and then relate it to what is known about main-sequence binaries. This has already been attempted for cataclysmic variables, but there are fewer unknowns for white dwarf binaries and we can hope to constrain common envelope evolution fairly directly.

T R Marsh, University of Southampton,
V S Dhillon, ING La Palma,
S R Duck, University of Oxford

UKSTU Facilities

The UK Schmidt Telescope Unit at ROE performs three major functions: an archive and lending library for UKST plates; the interface between all users (except Australian users) and the telescope; the copying of UKST plates and a general photography service.

Spectrum will be used to provide details of all these areas and any developments which might affect users. The following sets out basic details of the Plate Library at ROE and is expected to be mainly of interest to new users.

Plate Library at ROE

The Plate Library is set up both as an archive for all ROE's photographic plates and as an active library for UKST plates. The UK Schmidt Telescope has now taken over 16 000 original plates and films and the majority of these are stored in Edinburgh with others on loan to astronomers elsewhere. The telescope was operated by ROE from 1973 – 1988 and since then as part of the AAO. However, all plates should ultimately be stored at ROE although the AATB is the copyright holder for plates taken since 1988.

The UKST takes plates for southern sky surveys and on request for the research projects of individual astronomers. The good seeing (< 3 arcseconds) time is divided approximately equally between the surveys and individual research requests although this division can vary depending on the requirements of the surveys and highly rated non-survey programmes. All poorer seeing time is available for research programmes.

Applications for photographic material, for new material or to borrow existing plates, can be sent at any time to UKSTU, ROE. All such applications are assessed on receipt by the UK side of the Schmidt Telescope Panel but assessment of small applications has been delegated to ROE staff. Information can be obtained by e-mail by contacting **ukstu@roe.ac.uk**. The most significant recent development in the photographic capability of the UKST has been the routine use of Tech-pan film. This film is similar to IIIa-F but has a finer grain and goes about one magnitude deeper (in the *R* band) in the best conditions.

The complete catalogue of all plates taken with the UKST is held on computer at ROE. Many new research projects can be, at least, partially fulfilled from existing material. The plate catalogue can be interrogated by users – many users up to now have simply logged in to ROE and then typed the username/password UKSCAT. Under Unix this system of logging-in remotely will not be possible for the time being. However, one Vax is being kept at ROE and users will be able to use the program by logging in to UKSCAT on **revaxd.roe.ac.uk**. Any problems should be reported to UKSTU.

The Plate Library holds copies of all the major sky atlases; details are given in the table. Many of these atlases are being held on behalf of the whole UK astronomical community and are available for loan, consultation or measurement on one of the measuring machines. The original A-grade plates for the sky surveys being undertaken by the UKST are all held in a secure, fireproof safe room. These plates are not freely available for use or measurement. However, on receipt of an approved research application some of these plates may be released for measurement. This exception is usually restricted to those A-grade plates taken for a survey which is not yet being produced as an atlas.

The Plate Library is a national facility and was designed to provide facilities for visiting astronomers and short or long term visits are both welcomed and encouraged. The library is equipped with several light tables which are fitted with binocular microscopes. There is a polaroid camera for making instant finding charts although the recent acquisition of the CD-ROM set of Space Telescope measurements of the sky atlas plates is reducing the use of this camera. There is also a Packman *x-y* measuring machine which can be used to get positions accurate to about 1 arcsecond. Recent visitors include those hunting for lost asteroids or checking variable objects. Where a project requires the rapid inspection of a large number of plates a visit to ROE is easier for the user than the shipment of the plates to the user's institution. Visitors are asked to contact UKSTU in advance to ensure that the material required will be available.

The UKST also operates FLAIR, a multi-object fibre spectroscopic system. Details about this system will be given in future editions of *Spectrum*.

David Morgan, Sue Tritton, ROE

Atlas	Sky Coverage	Colour	Medium	Comments
POSS-I	Dec ≥ –30°	B & R	Glass	
POSS-I	Dec ≥ –42°	B & R	Paper	Including Whiteoak extension
POSS (I)	Dec ≥ 0° & $\|b\| \leq 10°$	I & R	Paper	
ESO B	Dec –90° – –20°	B	Film & Glass	
SERC (J)	Dec –90° – –20°	B_J	Film & Glass	
ESO (R)	Dec –90° – –20°	R	Film & Glass	
SERC I/SR	Dec ≤ 0° & $\|b\| \leq 10°$	R & I	Film	
SERC EJ	Dec –15° – 0°	B_J	Film & Glass	In production
SERC ER	Dec –15° – 0°	R	Glass	In production
SERC ER	Dec –15° – 0°	R	Film	Production planned
POSS-II	Dec ≥ 0°	B_J, R, I	Film & Glass	In production

Table 1 – Sky Atlases in the ROE Plate Library

Ipinfo

Telescope News

WHT Technical downtime on the WHT over the last ten months has continued at the 1993 level of approximately 4%.

A major upgrade to the UES A&G unit was carried out in September by a team from Roden (see the article below).

Commissioning of prime-focus imaging was completed in September, and was followed by two weeks of successful observing.

Autofib-2, the Durham-built robot fibre-feed for the WHT prime focus, had its first commissioning run in October. A full report appears on page 20 of this issue.

The flexure of the ISIS slit relative to the acquisition TV remains a problem. Tests with a dummy slit show that the flexure is somewhere in the A&G box.

The tower for the DIMM seeing monitor is now being erected outside the WHT. The monitor is already on-site and providing preliminary seeing measurements.

INT The telescope has been performing very well over the last three months, with little loss of telescope time due to technical problems.

Shack-Hartmann tests were performed in September at both prime focus and Cassegrain foci, and the optical performance of the INT is being fully characterised. Analysis of the optical aberrations is under way.

The filter offsets for prime focus imaging have been recalculated and tested successfully, thus solving a long-standing problem.

Grinding of the dome rail has resulted in a smoother motion of the dome.

JKT The telescope and control systems continue to perform well, with technical downtime below 4% during the last three months. CCD imaging runs constituted 60% of observing time during the period, and the RBS 30%.

TEK4 was successfully commissioned during July, although EEV still remains available. Single-windowing and binning (although not together), plus a choice of normal and quick readout speeds are available. Until the system has been fully defined, these functions are offered on a shared-risks basis.

Chris Benn, Emilios Harlaftis, Phil Rudd, ING La Palma

UES A&G Enhancement

In a joint effort with RGO Cambridge and La Palma at the end of September 1994, a small team from Roden installed an enhancement to the UES A&G unit, which allows offset autoguiding in almost all applications. Guiding by the observer and blind offsetting remain available for the cases where autoguiding proves impossible. With this basic enhancement now implemented, the way is clear for greater user convenience (and more efficient use of telescope time) by means of procedures which will more fully unify and automate the observing/data acquisition process. These procedures will involve computer star catalogues (*eg* The HST Guide Star Catalogue), the telescope, the A&G and the spectrograph. For instance, it is foreseen that ICL procedures will be implemented to automate the process of acquiring and guiding on a guide star. A no-derotator mode of operation, useful for faint point sources at high elevations, will also be brought into operation (note: no offset guiding possible in this mode). Contact Nic Walton on La Palma for details of progress (**naw@ing.iac.es**).

During the two commissioning nights in September, the autoguider performed successfully on stars down to magnitude, m_v = 16.2; at effectively m_v = 16.8, this faintest star was also accepted by the autoguider via the slitviewer channel (with closed slit). The seeing was good (in the range 0.5 – 1.0 arcseconds) and the near-full Moon was at high elevation. The fields available to observers on the monitor screen are now 17 arcseconds on a side in both autoguider and slitviewer channels. There is up to 50% vignetting for a few arcseconds at the edge of the field, for the rest of the field peak-to-peak variations of throughput are only 20%. The pixel size is of order 0.1 arcseconds, sufficiently small for the very best of seeing. The images of the fibres at the autoguider are of good cosmetic quality.

The absolute limiting magnitudes for guiding on the fibres have not yet been determined (a dark night is needed). But based on the figures obtained during the commissioning run in full moon, it is expected that guiding will be routinely possible down to 16.5 magnitudes, with objects visible to 17 magnitudes. Hence it is now possible to view most objects that may be observed by UES (down to m_v = 17) with the UES autoguider. Observers should note that both fibres have transmission only within the range 400 – 700 nm.

The enhancement to the UES A&G was carried out over a two-year period under contract to the Sterrenwacht Roden. It involved selection and testing of fibre image guides, relocation, redesign and rebuild of the autoguider CCD camera, rerouting of the image guides, redesign and rebuild of the image guide input facilities, upgrading the software of the autoguider VME computer and CCD controller and adaptation of the TCS software. Those involved in the design, construction and commissioning of the upgrade included (with apologies to those omitted): Mariet Broxterman, Geert Hagenauw, Arie de Jong, Alko Rijskamp (Roden); Palmera Arenaz, Jonathan Burch, Jaap Haan (ING); Bruce Gentles, Robert Laing, Sue Worswick (RGO). Thanks are also due to the technical support provided at the ING.

Jaap Tinbergen, Sterrenwacht Roden,
Nic Walton, ING La Palma

ING CCDs – End of One Era, Start of a New One?

It is now 10 years since CCDs first went into use on the ING telescopes, and so now is an appropriate time to review progress since 1984. We will therefore take this opportunity to bring our readers up-to-date with ongoing developments which we anticipate leading to significantly enhanced detector performance in the near future.

From 1984 onwards small-format GEC and RCA devices were installed, and these remained in regular use for many years. In 1989 new, larger format EEV devices were introduced, and these have recently been superseded by the more sensitive (thinned) TEK-1024 CCDs. We currently use these Tek devices on all telescopes, with minimal demand for the original, small format, CCDs (except those embedded in the FOS instruments). Within the last 12 months the original TEK1 head has been complemented by the TEK2, TEK3, TEK4 and TEK5 heads providing a full suite of thinned chips for all three telescopes. (In fact, at the time of writing TEK5 is being completed for installation by the end of 1994).

Whilst the TEK sensors offer excellent performance, we recognise the need to offer improved capability. For those who are unaware of our requirements here is a quick summary: larger focal plane areas (> 25 mm^2), small pixels (~15 μm), high quantum efficiency (thinned devices), and low readout noise (< 5 e^-). These options were reviewed last year (see Technical Note 92, November 93), and it was decided to adopt a dual approach to procure these sensors – this approach should offer flexibility and a greater chance of success.

Last year a 'foundry' batch of Loral 2k × 2k 3-edge buttable CCDs were ordered, and these were duly manufactured by February 1994. The yield was good (~60% functional), and gave us a useful set (~10) of potential devices which were then delivered to Mike Lesser at Steward Observatory to complete the crucial process of back-side thinning. The techniques involved in producing thinned chips are difficult and time consuming and delivery of our devices is overdue. Mike has recently achieved some success in thinning 2k × 2k 'Lick3' arrays, and we still anticipate successful completion of our devices any day. Watch this space, as they say.

As a second approach, we have been aiming to place a contract for the supply of a 'guaranteed' set of large-format CCDs from a commercial manufacturer (as opposed to a 'foundry' source). By the time this article is published we anticipate having placed a contract with the UK manufacturer, EEV. The AAO and Italian Galileo groups have joined with us as partners in this contract – which should yield six devices for the ING telescopes, in about 12 months time. These new arrays are similar to those being specified for Keck, Gemini and other large telescopes, and a summary of their specification is given below.

Proposed EEV/RGO CCDs

Format: 2048 × 4096 pixels. Size: 13.5 × 13.5 μm. 3-edge buttable.
Design: 2 outputs as standard; good signal linearity is specified.
Readout noise: $4e^-$ rms noise @ 50 kHz (spec), with an anticipated goal $2e^-$. Also, an anticipated noise of $5e^-$ rms @ 1 MHz pixel rates (goal).
Dark current: $4e^-$ $pixel^{-1}$ $hour^{-1}$ (goal is < $1e^-$).
Charge Transfer Efficiency:Serial & parallel CTE > 0.99999 (goal 0.999999).
Flatness: ± 15 μm deviation for the whole device.
QE (summary): > 50% @ 400 nm, > 75% @ 650 nm, good UV.
Good uniformity and blemish quality are also specified.

We are excited by the prospects of the enhanced capability that these new devices should offer in the near future on all our ING telescopes. We intend that they will give our spectrograph and imaging facilities state-of-the-art performance for all astronomical programmes. It should also be mentioned that there is a separate international project (RGO, Berkeley Lab, Roden) to develop a 4-chip mosaic imager for the INT prime focus. This system will also use Loral 2k × 2k CCDs, and is scheduled for completion at the end of 1995.

Paul Jorden, Paddy Oates, RGO

NOT

Under the arrangements set out in *Gemini* No 39, members of the PATT community are encouraged to apply for observing time on the 2.56m Nordic Optical Telescope (NOT) at the Observatorio del Roque de los Muchachos. Applications are currently invited for the allocation period that runs from April to September 1995. The deadline for this period is early in January. Proposal forms and further details can be obtained from the Director, Nordic Optical Telescope SA, Lund Observatory, Box 43, S-221 00 Lund, Sweden, e-mail **not@astro.lu.se**.

Service Nights, Semester 94B

Part or all of the following nights are available for the PATT and CAT Service Scheme on the ING telescopes, subject to schedule changes: D means dark; G, grey and B, bright nights.

WHT	ISIS/FOS/ Aux port	December 24 – 27 (G), 28 (D), January 2 (D), 22, 23 (G)
	UES/ISIS	December 9 (G), 15 (B), January 16 (B)
	Prime focus (imaging)	December 1 (D)
INT	IDS/FOS	December 12 (B), 27 (G), 28 (D), January 1 (D), 9, 10, 18 (B)
	Prime focus (imaging)	January 24, 25 (G)
JKT	CCD imaging	December 12, 21 (B), January 11, 19 (B), 22 (G)
	Photometer	December 13 (B)

Service requests should be for not more than 3 hours, including calibration.

Service requests should be sent to the account **service@mail.ast.cam.ac.uk**. A form can be obtained by anonymous ftp from the Cambridge SUN cluster (**cast0.ast.cam.ac.uk**) where it is held in the directory /public/ftp/service. Updates on the status of Service observing programmes can be found in LPINFO under **Service_Obs**.

Bill Martin, RGO

The ING Documentation System

The ING paper documentation system consists of the ING La Palma Observers Guide, a series of User Manuals and a series of Technical Notes.

The object of the Observers Guide is to provide sufficient information about the ING telescopes and their associated instrumentation to allow an astronomer, *eg* to prepare an observing programme proposal. It also provides general information about La Palma and facilities on site. The current version is 2.0, November 1988, and a new version is expected to appear in 1995.

The series of User Manuals explain in greater detail how to use individual instruments and associated software. The Technical Notes deal with a wide range of topics related to observing on La Palma.

The full list of current Manuals and Technical Notes is given in the Users Documentation Guide, available from Bill Martin at the RGO Cambridge (**wlm@mail.ast.cam.ac.uk**). The list is also available via the LPINFO on-line HELP system and the La Palma information pages of the World Wide Web information service (see *Spectrum* No 3, page 13). The following Technical Notes have recently appeared.

94
W L Martin (RGO)
ING Bibliography, 1993 (March 1994)

95
J Pilkington, J Sinclair, R Wood (RGO)
Landolt Faint Photometric Standards (July 1994)

Bill Martin, RGO

First Light with Autofib-2

Following exhaustive tests in Durham and at RGO, the Autofib-2 robotic fibre positioner (AF2) was successfully commissioned at the WHT prime focus during a 10-night run in October. Rather more than 50 percent of the time was lost due to adverse weather conditions.

The tests carried out in the UK had already demonstrated that absolute fibre placement accuracy under all normal operating conditions is better than 15 μm (0.25 arcseconds). During the run, a full set of fibres (6 guide fibres and 118 spectroscopic fibres) was operated for the first time. By carrying out several field set-ups, AF2 automatically learned the error tables for the new fibres, and the excellent positioning performance seen in the UK was recovered on the telescope. A set-up time of 10 seconds per fibre (as for the UK tests) was achieved on the WHT, so full field set-ups took 20 to 25 minutes.

The emphasis of the commissioning tests was to establish the exact transformation required between sky positions and AF2 (x,y) coordinates so that each fibre can be precisely placed on its target. This involves knowledge of the geometry of the prime-focus field as imaged through the corrector. Initially, the information was determined from measurements of prime-focus plates taken in April. To refine the transformation as it applies to AF2, the robot itself was used to measure the positions of stars in the field. It can do this very accurately because it has two sky-viewing probes: one which can access the whole field, while the other is used to autoguide on a star at the edge. Towards the end of the run this mapping process was providing a fit with rms residuals of only 0.35 arcseconds.

The six guide fibres feed light from guide stars to a Westinghouse TV, and these were used to give an initial rough estimate of how accurately the fibre configurations could be aligned with the target fields. After fine-tuning the telescope pointing and field rotation, individual guide fibres showed residuals of less than an arcsecond. It was also demonstrated that field acquisition was straightforward and could be done in under a minute.

The Autofib-2 robotic fibre positioner has been successfully commissioned at the WHT prime focus.

In the absence of the WYFFOS spectrograph (which is scheduled to be delivered in March 1995), the light from the spectroscopic fibres was simply imaged with an 85 mm SLR camera lens through a V filter onto EEV6. Fibre images of flat fields (dome and sky) were obtained for comparison with lab throughput results obtained earlier. Fibre images of target star fields were also taken, and a preliminary inspection clearly indicated that starlight was coming down the fibres. These data are currently being reduced to determine the accuracy with which the fibres were placed on the stars.

AF2 performed reliably throughout the run and all aspects of its operation were tested. The daytime jobs of putting it on and taking it off the telescope are quite complex procedures. They went relatively smoothly, however, and no particular difficulties are foreseen in carrying them out routinely. Remaining work on AF2 consists mainly of tidying up a few loose ends in both hardware and software. The instrument will be formally handed over when WYFFOS is commissioned next year.

Those involved with the manufacture and commissioning of AF2 were: Shetha Al-Dargazelli, Phil Armstrong, Stuart Barker, Terry Bridges, Jonathan Burch, Esperanza Carrasco, Andrew Colville, George Dodsworth, Dave Gellatly, Bruce Gentles, Billy Hogg, Lewis Jones, Steve Lishman, Kevin McGee, Chris Moore, Paul Morell, Ken

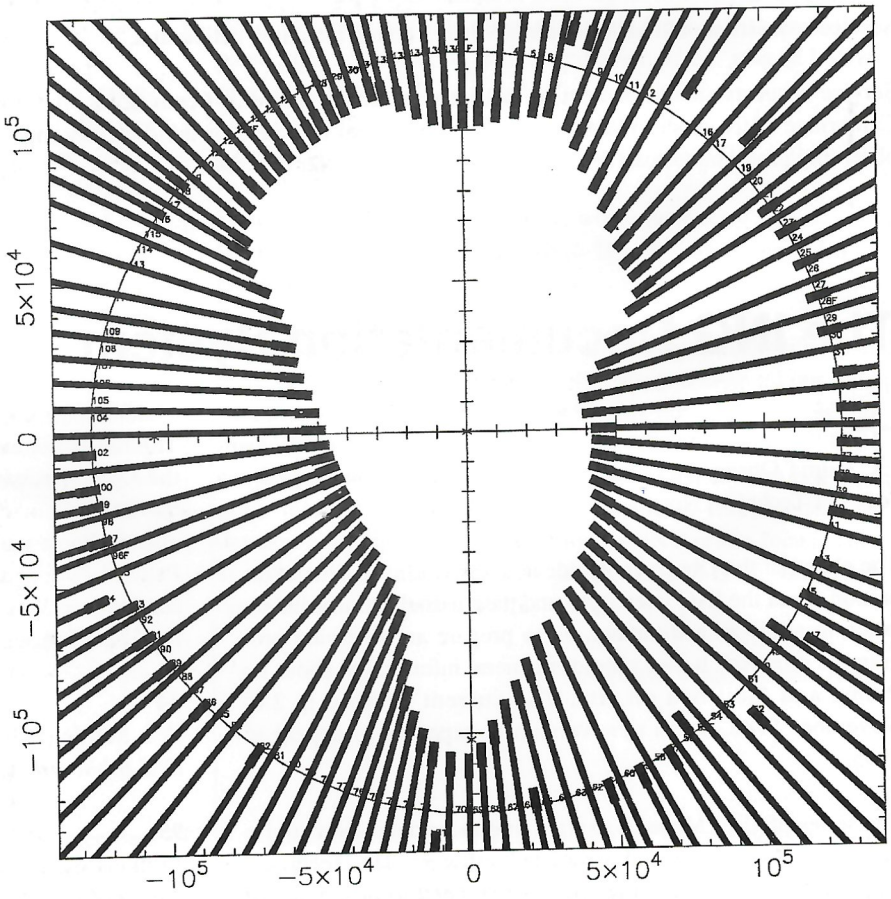

Fig. 1 – Graphic display from CONFIGURE, an interactive off-line program used to allocate fibres to target objects. The map of La Palma was, in fact, set up by the robot as part of the reliability testing, and an rms accuracy of 5 μm (or about 1 metre in the real thing) was achieved.

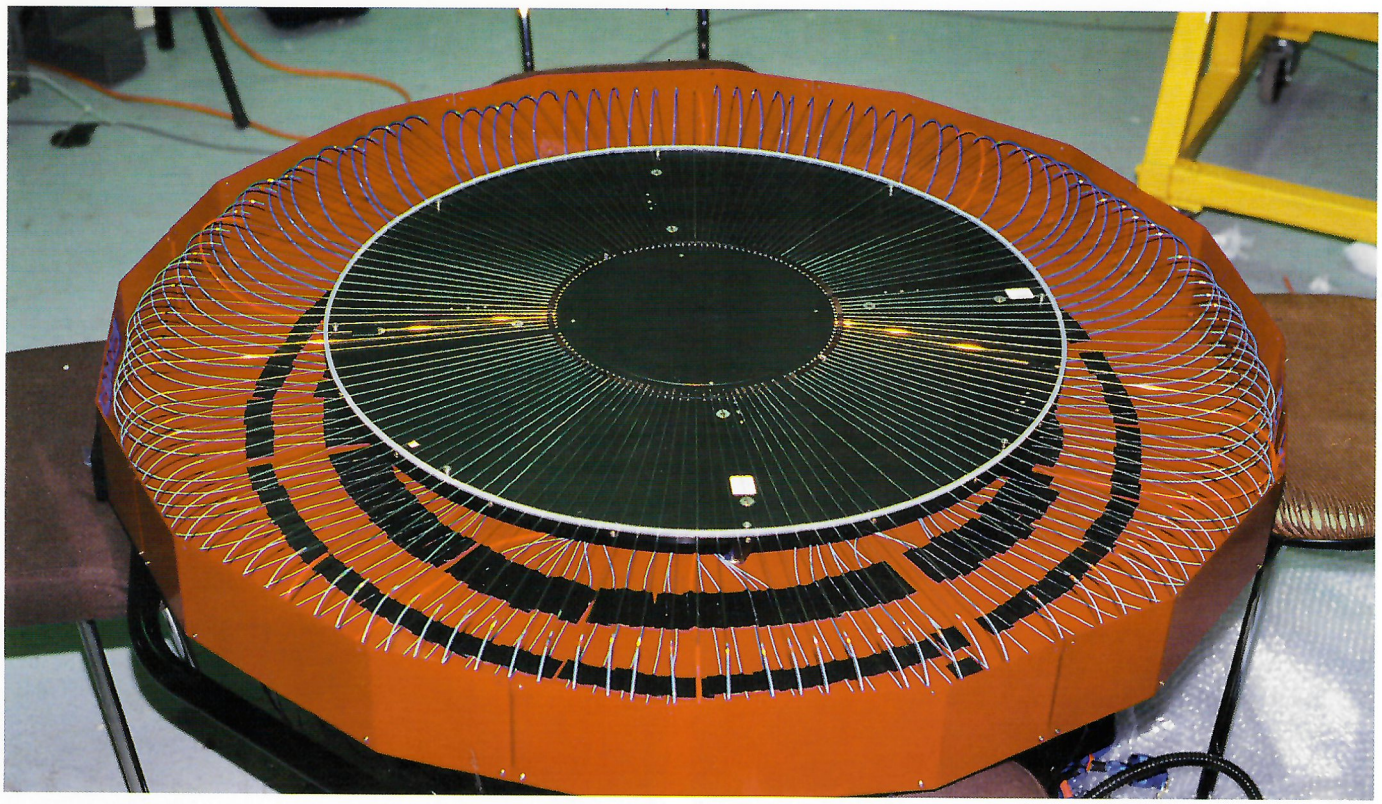

Fred Watson

Fig. 2 – Looking like some giant exotic flower, the Autofib-2 fibre field-plate assembly awaits its protective cover before being loaded onto the telescope. The fibres radiate from their 'park' position at the edge of the 200m diameter field-plate (centre) in stainless steel rods before looping behind to emerge in protective cables for the run down to WYFOS.

Parkin, Paul Rees, Ray Sharples, George Teasdale, John Webster and Tim Wilkins.

The commissioning team would like to thank the La Palma staff for all their help and support throughout the run. Thanks also to Bob Argyle, Dave Carter, Kyle Cudworth, Nick Ferneyhough, Mike Irwin, Mick Johnson, Robert Laing, Paul Martin, Chris McCowage, John Pilkington, Janet Sinclair, Howard Stevenson, Percy Terry, Nic Walton, Andy Weise and Sue Worswick.

Ian Parry, Anglo-Australian Observatory,
Ian Lewis, University of Durham,
Fred Watson, RGO

Crawford Exhibition at the Royal Museum

On the evening of 6 October 1994, around one hundred guests gathered in the Royal Museum of Scotland for the official opening of the *Heavenly Library* exhibition. Following short speeches by Mark Jones, the Director of the Museum, and Stuart Pitt, ROE, Professor Arnold Wolfendale, who had been invited to open the exhibition, took up his position on the steps outside the exhibition room to address the guests. His entertaining speech included references to the wine (of which there was an ample supply), and questioned what the original benefactor, the 26th Earl of Crawford, would have thought of the present Astronomer Royal for the southern half of the kingdom opening an exhibition celebrating a collection that saved the Royal Observatory in the northern half of the kingdom!

With the speeches complete, the guests eventually entered the exhibition room to admire some of the treasures of the Crawford Library, which was displayed alongside instruments from the Science Museum, London, the National Museums of Scotland and St Andrews University. Comments made during the evening, and over the following weeks by members of the public, confirm that this truly is a splendid exhibition. Along with such treasures as first editions of Copernicus and Euclid, there was one cabinet devoted to non-astronomical books, including some from the 16th century on the art of waging war!

B W Hadley

After a year containing a variety of events to celebrate the Centenary of the Royal Observatory on Blackford Hill, the saviour of the Observatory one hundred years ago has also provided a superb finale to our centenary celebrations.

Mark McAuley, ROE

Near Infrared Imaging of IRAS Galaxies

Recent studies of the nature of ultraluminous IRAS galaxies (ULIRAS) indicate that these objects are in fact gas rich ellipticals in the process of formation by merger-induced dissipative collapse. It is further proposed that the ULIRAS galaxies are an evolutionary stage of mergers of dust rich spirals, evolving into elliptical-like objects. Therefore, it is possible that once dust is swept away from their nuclear regions, by the combined forces of supernova explosions and radiation pressure, these objects will take on the appearance of normal ellipticals.

High resolution near infrared imaging of ultraluminous IRAS galaxies is being used to study galaxy mergers.

This scenario is supported by measurements of typical gas densities in ULIRAS galaxies, which are found to be as high as the stellar mass densities in the cores of ellipticals, and by the *V*-light profile of merger galaxies which are shown to follow the de Vaucouleurs $r^{1/4}$ law for ellipticals. However, in most merger candidates, the optical structure is contaminated by bursts of star formation and extinction by dust lanes. The near-infrared (2 μm) light of galaxies is largely unaffected by extinction, population mix and star formation effects and is mainly dominated by old stars, formed well before the mergers. Therefore, the idea that ULIRAS galaxies are an evolutionary stage of mergers

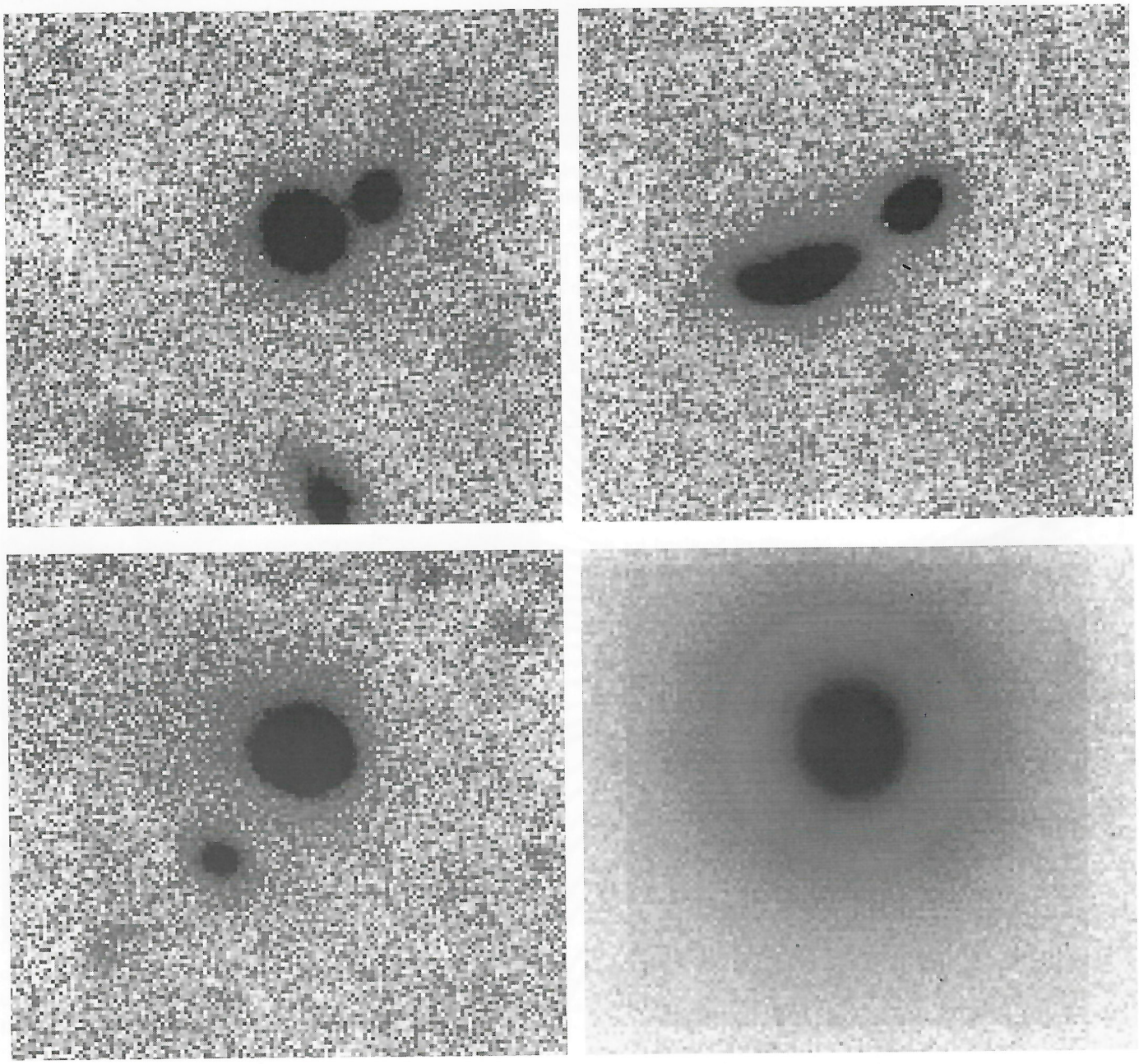

Fig. 1 – Reduced K-band IRCAM3 images of ultraluminous galaxies IRAS 1420 (top left), IRAS 1516 (top right), IRAS 1604 (bottom left) and an elliptical galaxy N4874 (bottom right).

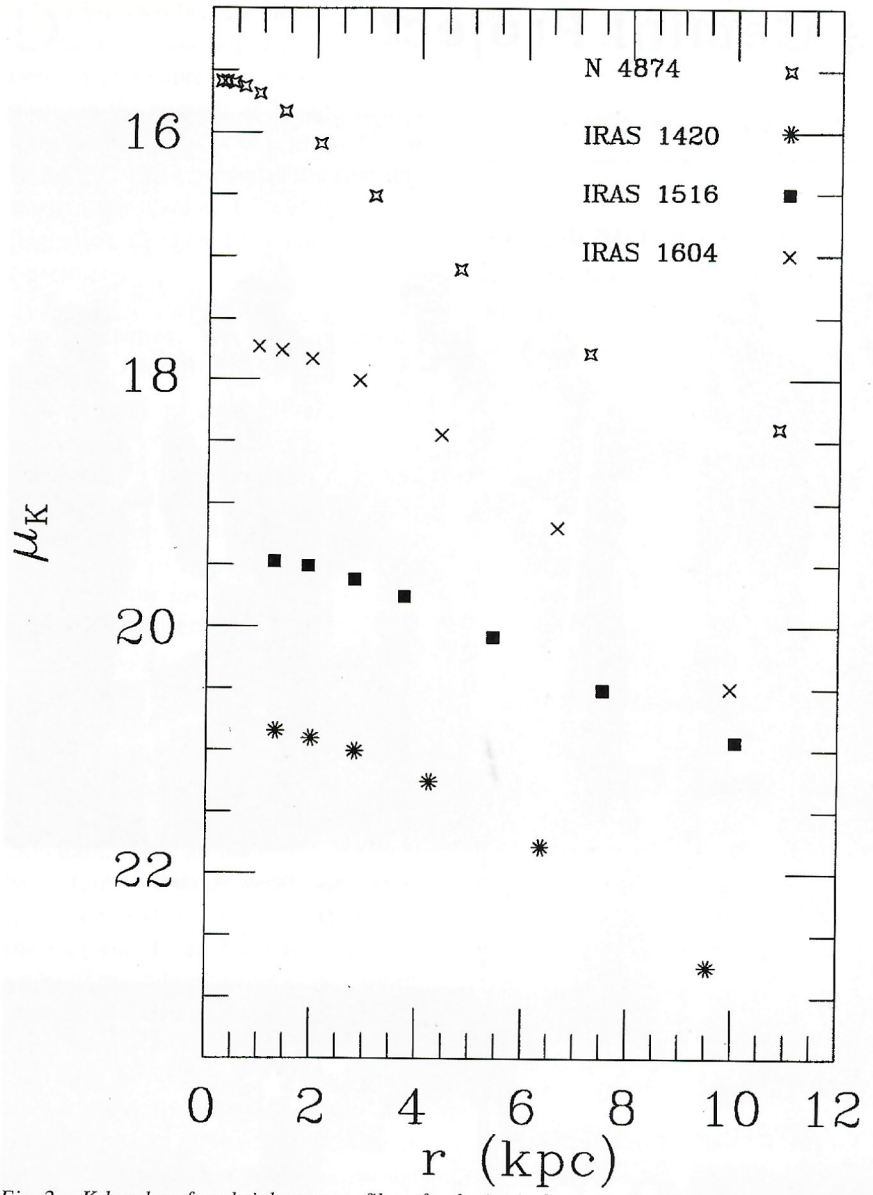

Fig. 2 – K-band surface brightness profiles of galaxies in figure 1. For the purpose of comparison, The profiles are arbitrarily normalised in surface brightness. A value of H_0 = 50 km/sec/Mpc is used.

of spirals evolving into elliptical galaxies can be tested by investigating whether their *K* brightness profile obeys the $r^{1/4}$ law.

High resolution, near-infrared (2.2 μm) observations of a number of ULIRAS galaxies and normal ellipticals were carried out, using the United Kingdom Infrared Telescope (UKIRT) and IRCAM3 (a 256 × 256 detector array with a pixel size of 0.286 arcseconds). The sample of ULIRAS galaxies in this study is selected to include galaxies in their initial (IRAS 1516) and final (IRAS 1604) stages of mergers as evidence from their optical (*R*-band) images. A total integration time of 30 minutes was used for the ULIRAS galaxies and 10 minutes for the ellipticals. Images of galaxies were taken alternately with nearby regions of blank sky which were subsequently used to form the flat field. After dark current subtraction and flat fielding, the mean sky brightness on the image frames was measured and subtracted. The images were calibrated using observations of standard stars. Reduced IRCAM3 images of three ULIRAS and an elliptical galaxy are presented in figure 1. Surface photometry was carried out on these images, using the RGASP package in the STARLINK environment. The main source of error in the derived surface brightness profiles arises from the systematic uncertainty in the sky level. The errors in surface photometry were estimated, using the standard deviation of the sky counts on independent images.

The *K*-band surface brightness profiles of the ULIRAS galaxies are compared in figure 2 with that of the elliptical galaxy N4874. The IRAS 1516 galaxy, which from its morphology (figure 1) appears to be in the initial stages of mergers, has a *K*-band profile significantly different from ellipticals and more similar to that of the spirals presented in Wright *et al* (*Nature*, **344**, 417, 1990). However, in the case of IRAS 1604, which is an isolated galaxy presumably in its post-mergers phase, the rate of change of the *K*-band surface brightness with radius resembles that of the ellipticals (figure 2). Moreover, the far-infrared (60 μm) flux of this galaxy is smaller than those in the process of mergers (IRAS 1516 and IRAS 1420), supporting the evidence from its morphology and *K*-band surface brightness profiles that it is a relaxed, elliptical-type object, having lost most of its dust content. The IRAS 1420 galaxy is in an advance stage of mergers and has a higher 60 μm flux than the other ULIRAS galaxies in figure 2, implying that it has not yet been depleted of gas. Compared to IRAS 1516, the *K*-band surface brightness profile of this galaxy is closer to that of the ellipticals.

The similarity of IRAS 1604 to elliptical galaxies is further supported by the size of its effective radius, containing half the *K*-band light, which is found to be 3 kpc (using H_0 = 50 km/sec/Mpc) as measured from the best fit de Vaucouleurs law. This is consistent with the effective radius measured for N4874 here and with other ellipticals. However, in the case of IRAS 1420 and IRAS 1604, the effective radius is higher (~3.8 kpc), suggesting a more extended distribution of the near-infrared light in these objects.

This study has shown that the *K*-band surface brightness profiles can be used as diagnostics to identify the state of mergers of ULIRAS galaxies and hence, to explore whether these objects are an evolutionary stage of mergers of spirals to elliptical galaxies. The results here are consistent with the observed morphologies of these galaxies and their far-infrared 60 μm fluxes. Any such scenario must ultimately account for the removal of interstellar material from galaxies. It is expected that supernova explosions can provide sufficient mechanical energy to deplete these galaxies of gas.

Bahram Mobasher, ICSTM

Landmarks for the Gemini Project

Fig. 1 – Participants at the Mauna Kea ceremony using traditional Hawaiian implements in the Gemini North groundbreaking ritual.

Fig. 2 – The flags of the six partner nations of the Gemini project, marking the site of the pier of Gemini South, at Cerro Pachon.

During October the Gemini Project took several important symbolic steps. A groundbreaking ceremony took place on the summit of Mauna Kea, a foundation stone was laid on Cerro Pachon, Corning produced the first primary mirror blank and Chile, Brazil and Argentina all signed the International Agreement.

On 7 October, Mauna Kea guests including Alec Boksenberg and local staff gathered in perfect submillimetre observing weather. In the Hawaiian culture land called *aina* is held in trust and used thoughtfully, not owned to be exploited. In his introduction to the day's Master of Ceremonies, Don Hall, Director of the Institute for Astronomy, stressed our sensitivity to this. A Kahuna Kepa Maly honoured the ground and recognised the traditional Hawaiian god Lono and the goddess Poliahu who inhabits the adjacent peak of Pu'u Poliahu having banished the goddess of fire, Madam Pele from the mountain. After an address in English he performed a magnificent and evocative chant in Hawaiian. As Chairman of the Gemini Board Malcolm Longair spoke of the cultural benefits that use of the site for astronomy would bring to all mankind. He also thanked all of those who had worked at the international level to make the project possible. Both the Governor of Hawaii and the Mayor of the County of Hawaii articulated the economic, educational and cultural benefits which astronomy had introduced to Hawaii. The Gemini Project Director welcomed all of the international partners to a project which would challenge the scientific and technological abilities of all of them. Joao Steiner of Brazil stated that some of his colleagues in Brazil had some trepidation about Brazil entering straight into big league astronomy. But in his opinion a country that had the commitment to win the football World Cup had the dedication to succeed in its chosen fields.

Groundbreakings have a special significance in Hawaii: not only should the ground be blessed but prayers for the safety of those who will be working on the site are essential. Monsignor Kekumano offered these prayers and completed the blessing by pouring holy water on the ground. Formal breaking of the ground followed: the principal participants in the ceremony used o'o sticks, traditional Hawaiian implements, to initiate the excavation.

Several important advances were achieved in October by the Gemini twin 8m telescope project.

In late October the Gemini Science Committee (GSC) met in Chile for the first time to see Cerro Pachon, learn first-hand about the qualities of the site and meet the CTIO staff. AURA had arranged that the ceremony to lay a foundation stone should take place the day after the GSC meeting so there was

an air of celebration and anticipation surrounding the proceedings. Much of the first day of the meeting was taken up with reports of progress in the project and a wide ranging discussion of the pros and cons of "queue" scheduling. At the end of the first day the GSC learned (to much applause) that Chile had added its signatures to the International Agreement. The second day was devoted mostly to reports from the three instrumentation working groups set up to monitor progress with adaptive optics and acquisition and guiding, infrared and optical instrumentation. Meanwhile Dick Malow, AURA's special assistant for Gemini, took the agreement to Argentina and returned with the final signatures on the document. This was the perfect prelude to the events of Saturday and concluded the GSC's meeting on a high note.

The subsequent ceremonies took place on 22 October, a warm spring day if rather cloudy. The journey to Cerro Pachon involves about a 90 minute drive from La Serena, and when the convoy of buses finally reached the summit, it was possible to see the enormous changes that had taken place. The small knoll at the summit, and the meteorological tower at its peak, had been blasted away to produce a flat topped ridge. Painted on this was an enormous circle about 30 m in diameter to represent the size of the enclosure. In the centre was another ring, the size of the pier, with the flags of the 6 partner nations around the circumference. The formal proceedings, managed by Malcolm Smith (Director of CTIO), were brief. Malcolm Longair said a few inspiring words describing the cultural significance of the science to be pursued from Pachon, and representatives of Chile and Brazil also spoke. The site was blessed by a priest who said a prayer for the safety of the construction workers. Malcolm then lowered the stone into place and everyone returned to CTIO for a celebratory lunch.

Guests at both groundbreakings were presented with samples of the ULE glass from the boules used to make the Gemini mirrors. The most impressive technical milestone in October was the fusing of the hexagons to produce the first Gemini blank, a virtually flawless disk of ULE glass.

Those of us working on the Gemini project have been caught up in its increasing momentum. The formal groundbreakings and the final signatures on the international agreement signal the need to expose more of our community to the project. For some time, scale models of the two 8 m telescopes have been under construction. The events in October spurred them to completion. One model will be in the UK by the end of the year. We can put it on display for the astronomy community to see. Whether it's the Northern one or the Southern remains to be seen!

Roger Davies, UK Project Scientist,
Terry Lee, UK Project Manager

Redshifts of Flat Spectrum Radio Sources

VLBI observations have revealed a variety of structures in active galactic nuclei (AGN). These range from asymmetric core-jets – which often show superluminal motion – to compact symmetric objects (CSOs) – some of which look like Cygnus A but on a scale 1000 times smaller – to the convoluted structures observed in some compact steep spectrum sources (CSS). To clarify the relationships between the various types of source one can either study a few representative objects in detail or well-defined samples of sources to investigate their statistical properties.

So far, due to limited observing time, the first approach has dominated VLBI efforts. The largest complete sample available has been the 'PR' sample of Pearson and Readhead (Caltech) which contains 65 objects (flux density limit $S_{6cm} > 1.3$ Jy), 45 of which were suitable for imaging with the narrow-band Mk2 VLBI system. The large number of apparently different classes of AGN, as revealed by PR's analysis, prompted us to expand their work by making observations of much larger complete flux-density-limited samples of radio sources. The programme is a collaboration between the California Institute of Technology (Caltech) and NRAL Jodrell Bank (University of Manchester) and hence our two surveys are identified as the first and second Caltech-Jodrell Bank or CJ1 and CJ2 surveys. The CJ1 survey extended the PR survey down to $S_{6cm} \geq 0.7$ Jy; it contains 135 sources of which 82 could be mapped with Mk2 VLBI. The PR and CJ1 samples were selected at λ6 cm and hence mostly contain objects where the dominant radio emission arises in a flat-spectrum component. The CJ2 survey extended the flux limit further down to $S_{6cm} \geq 0.35$ Jy and contains 187 sources, all of which have been mapped with VLBI. In contrast to the PR and CJ1 samples, the CJ2 sample was explicitly restricted to sources with integrated spectral indices flatter than –0.5 (where $S_\nu \propto \nu^\alpha$).

During the course of the CJ1 and CJ2 surveys from March 1990 to late 1993 we made almost 400 VLBI images of AGN principally at λ6 cm (resolution ~1 milliarcsecond) but, for the CJ1 sample and some of the PR sample, at λ18 cm as well (resolution ~3 milliarcseconds). Because we were able to employ 12 – 17 telescopes in the global VLBI array we used a 'snapshot' observing technique allowing us to observe ~20 sources per day. The CJ surveys are by far the largest VLBI surveys carried out to date.

An extensive VLBI survey is being followed up by a programme of spectroscopy.

Cosmological goals

As well contributing to our understanding of the properties of compact radio sources and their evolution with cosmic epoch, our VLBI surveys had three explicitly cosmological aims.

Kellermann and Gurvits have independently suggested that the milliarcsecond angular size *vs* redshift ($\theta - z$) diagram provides a new test of universal geometry which may well be free of evolutionary effects that confuse the larger scale angular size-redshift relation. Our new homogeneous body of VLBI data is clearly important for this test.

Cohen and Vermeulen have shown that the superluminal motion vs redshift ($\mu - z$) diagram shows a clear trend of decreasing angular speed with z which is consistent with standard cosmologies with q_0 in the range 0.05 – 0.5. VLBI monitoring observations of CJ1 and CJ2 sources should yield 100 – 200 additional superluminal sources for this analysis, enabling q_0 to be determined to ± 0.1.

Our VLBI surveys are sensitive to gravitational lensing on scales of 1 – 100 milliarcseconds corresponding to lensing masses in the previously unexplored range of $10^6 - 10^9$ solar masses. Of particular interest in this range are pregalactic compact objects (PCOs) which arise in a wide range of cosmogonic scenarios with a mass scale of $10^{6.5}$ solar masses. We have not yet found any 'milli-lenses', although there remain a few candidates which we have not yet definitely ruled out. If there are no milli-lenses in our samples then PCOs must constitute less than 1% of the closure density.

The INT observations

For all our astrophysical and cosmological programmes full redshift information is necessary to extract the maximum information from the VLBI data. The redshift information for the complete PR and CJ1 samples is now over 90% complete, thanks in no small measure to our Caltech colleagues' (Readhead, Pearson and Xu) observations at Palomar, but before 1993, only about 25% of the CJ2 objects had known redshifts. During 1993/94, therefore, we spent two dark weeks using FOS on the INT to obtain redshifts of CJ2 sources. We observed all CJ2 sources that had optical counterparts on POSS, typically for 3000 seconds per object.

Whereas one of us (IB) had long experience in this field, two of us (DH and PW) were complete beginners. It turned out that the fates were kind to us. Not only did the INT/FOS combination work flawlessly during our 14 nights but about 80% of the time was clear. As a result we were able to observe ~100 CJ2 sources with an overall success rate for obtaining redshifts of ~60%. For VLBI observers used to obtaining their data months after observation and then having to embark upon a lengthy reduction process, the 'buzz' associated with successful optical observing was noticeable. It was great fun to be able to get the basic results almost in real-time using the local ADAM-based software and a calculator.

Most of the objects were acquired simply from APM finding charts kindly supplied by Richard MacMahon at IoA Cambridge. However, before obtaining these, IB had visually examined all the CJ2 fields on the POSS prints. Gratifyingly there was very good agreement between the by-eye and the machine-generated results but it was nice to have both. Close to the plate limit the APM produces more reliable identifications and magnitude estimates but it can be confused by merged images which the experienced eye can deconvolve. Indeed one of our highest

redshift quasars was only correctly identified by eye.

Current redshift statistics

Following our INT runs most of the bright CJ2 sources ($m_r < 19$) now have redshifts. The great majority are quasars but a significant minority of the bright objects (~10% of our INT sample) have featureless BL Lac-type spectra. We had difficulty obtaining redshifts of the fainter objects ($m_r > 19$) and indeed most POSS empty fields (~20% of the CJ2 sample) were not observed at all. Our Caltech colleagues Vermeulen and Taylor have recently continued the CJ2 redshift programme by observing ~30 of the faint objects (including EFs) on the Palomar 5m. As a result of these efforts the redshift-completeness of the CJ2 sample has now increased to ~70%.

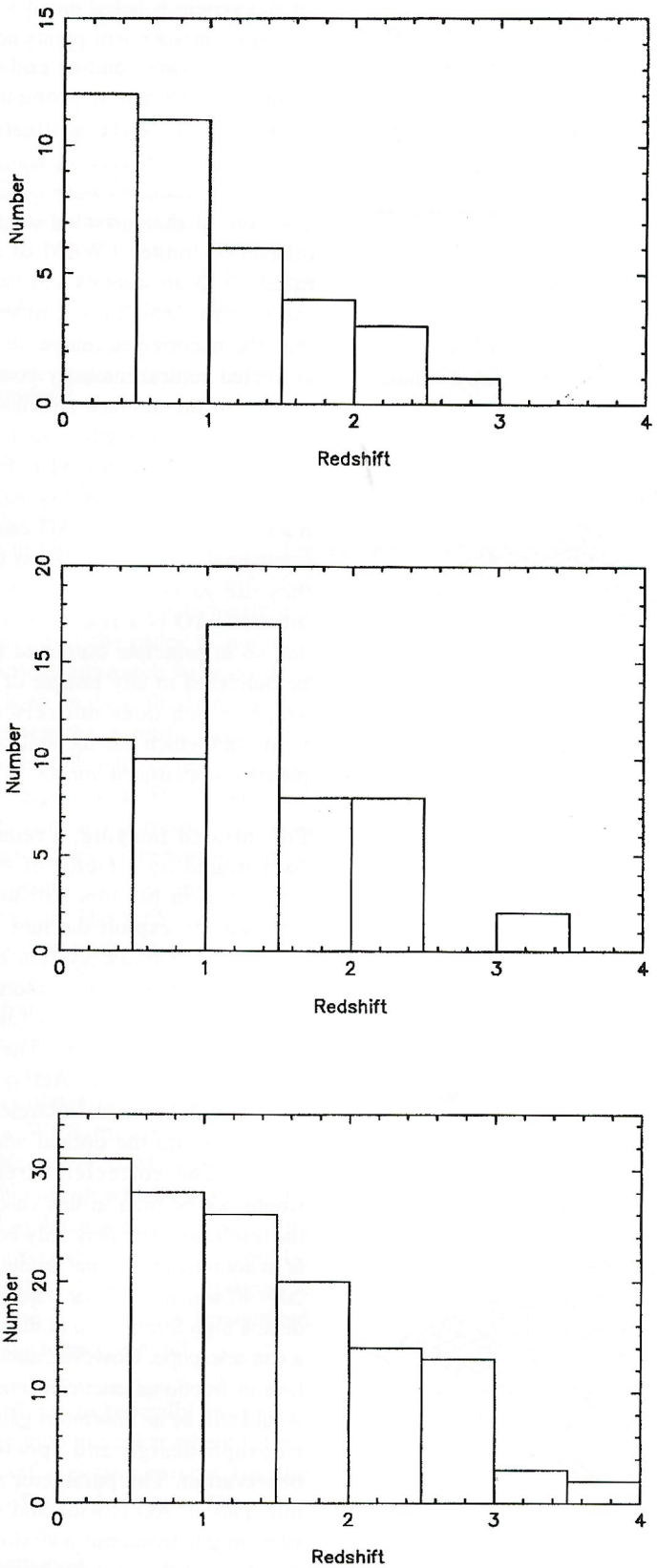

Fig. 1 – Redshift distribution of top: PR flat spectrum sources ($S_{6cm} > 1.3$ Jy); middle: CJ1 flat spectrum sources ($1.3\,\text{Jy} > S_{6cm} > 0.7$ Jy); bottom: CJ2 sources ($0.7\,\text{Jy} > S_{6cm} > 0.35$ Jy).

The current redshift statistics of the flat spectrum radio sources in the PR, CJ1 and CJ2 samples are shown in figure 1. The fraction of high redshift sources is a surprisingly strong function of the limiting flux density of the sample. In the combined PR and CJ1 samples only 3 objects (~3%) have $z > 2.5$ whereas in the CJ2 sample there are so far 18 objects (~9%) with $z > 2.5$. Currently the mean redshift of the CJ2 sample is 1.42 and the highest redshift object has $z = 3.89$.

Although we now have a good idea of the redshift statistics of the CJ2 sample, it is biased by the lack of redshift information on the optically fainter sources. These may be the highest redshift objects and so affect our interpretation the most. We have therefore proposed to observe the 42 remaining CJ2 sources without redshifts (mostly EFs) on the WHT. Our goal is to increase the redshift completeness of CJ2 from the current ~70% to about 90%; the redshift completeness will then be comparable to that of PR (100%) and CJ1 (88%). With our extensive radio and optical data we will then have by far the best studied sample of flat spectrum radio sources in the northern sky.

Acknowledgements

Richard MacMahon and Isobel Hook (IoA Cambridge) provided a lot of help in this work. Not only did they supply us with the APM identification charts and advice about observing strategies on the INT, they subsequently taught DH how to use IRAF to carry out the optimal extraction of the spectra. Next time however, we hope that they will arrange increased security for the IoA computers, many of which vanished while these data were being reduced!

David Henstock, Ian Browne,
Peter Wilkinson,
University of Manchester

Adaptive Optics for the WHT and UKIRT

The UK adaptive optics (AO) programme is funded to provide common-user AO at WHT GHRIL in 1997 and at UKIRT in 1998. This article describes the projected gains that these systems should deliver, their methods of operation and the timescales of the programme.

The purpose of AO is to improve image quality by reducing the optical effects of turbulence in the air above each telescope. This turbulence evolves continuously and so its effects, the seeing, can only be compensated by dynamic and generally small elements downstream of the telescope primary mirror. In this respect, AO is distinct from active optics which removes slowly changing errors in the figure and alignment of the telescope optics.

The UK adaptive optics programme will deliver significantly improved image quality to the WHT and UKIRT in the next few years.

The projected gains

The potential gains from AO are illustrated in figure 1 which shows a simulation of a system working on the WHT. The before and after images are in the *K*-band and have been simulated under rather good starting seeing (0.5 arcseconds in the optical). The simulated AO system is based on an 8×8 grid of phase measurement points across the pupil and a corresponding grid of phase actuators. The actual geometry when applied to the WHT is illustrated in figure 2.

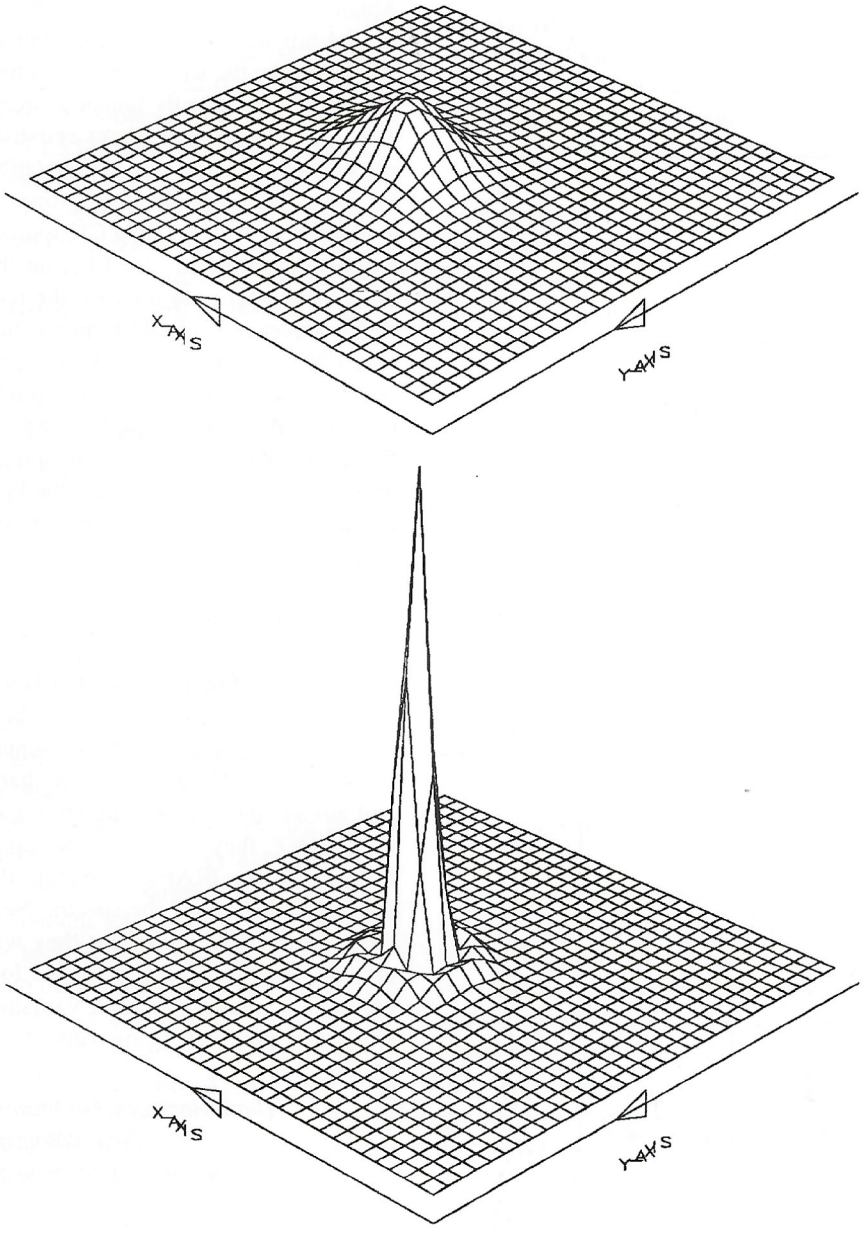

Fig. 1 – Simulated K-band images at WHT before and after adaptive correction.

The core of the corrected image has a diffraction-limited FWHM of approximately 0.13 arcseconds and has a central intensity which is six times greater than the uncorrected image. In fact, the corrected central intensity corresponds to 67% of the ultimate attainable intensity at this wavelength. This fraction is called the Strehl ratio and is frequently used as a measure of AO system performance. The gains from AO can be very substantial and for a 4 m class telescope they are easiest to obtain in the near infrared. AO is a real-time technique and so in principle corrected light can be delivered to any imager or spectrograph which does not rely on wide fields and which has the ability to sample the compensated images.

For infrared imaging, a reduction in background by a factor of ~15 is an obvious gain but this will not be the only way to exploit the new AO systems. Our example system could, in addition, deliver gains at shorter wavelengths by exploiting a fairly new avenue of AO technology. The aim is to use such 'low-order' AO systems to provide reductions in encircled energy radii well into the optical wavelength region. The corrected Strehl ratios would not be high in this case because the resolution gain may only be ~5. This is in contrast to the sharpening factor of 20 – 40 which would be required to produce a high Strehl ratio in the optical on a 4 m telescope. However, such a reduction in fractional encircled energy radii would still be an enormous gain to spectrograph design and spectroscopic observation. The parameter space for this 'partial' AO is wide and we would very much welcome a dialogue with members of the community who would benefit from the optimisation of a par-

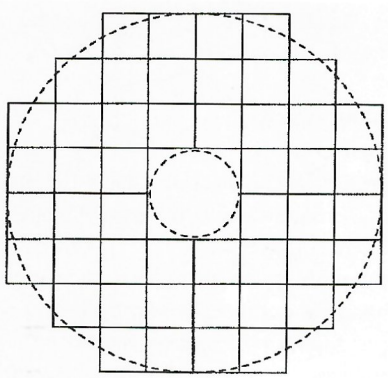

Fig. 2 – The simulation wavefront sensing and actuation geometry projected onto the WHT primary. Each of the small squares is one corrective degree-of-freedom.

ticular image parameter or who would like to suggest a new application of the technique.

AO technology

A generic AO system is illustrated in figure 3. The key components are: *the wavefront sensor* (WFS), which measures the instantaneous wavefront phase deformations. For a 4 m telescope, the RMS changes in optical path length due to seeing are of the order of microns. The simplest approach to wavefront sensing is to analyse the light from a guide star near the scientific target, or, if it is sufficiently bright, some of the light from the target itself. The actual measurements normally correspond to local wavefront slopes or curvatures at an array of points over an image of the telescope pupil. The WFS can operate at shorter wavelengths than the science instrument so when the science goal is in the infrared we can use visible light to do the wavefront sensing; *the reconstructor*, a powerful real-time computer which calculates the wavefront shape from the WFS measurements; *the deformable mirror* (DM) which is generally a thin mirror which can be rapidly refigured by force actuators driven from the reconstructor output signals. Typically the DM is 100 – 200 mm in diameter and is placed at a demagnified image of the telescope pupil.

A practical system generally has a separate image motion tracker which is used with a fast steering mirror for the removal of wavefront tilt. Tilt is the dominant component of turbulent wavefront deformation.

Factors affecting AO performance

Whilst appreciating the potential of AO on the 4 m telescopes, we must also assess its limitations. The performance of AO is dependent on both the observational wavelength and the seeing environment. Let us examine the effects of a change in seeing on the corrected image in figure 1 which was simulated in half-arcsecond visible seeing with a $V = 17$ guide star. If we changed the seeing to one arcsecond, we would produce a similar image core but the Strehl ratio would be reduced to 32%. We could restore it to ~70% by increasing the guide star brightness to $V = 14$ but this would mean reduced sky coverage. Alternatively we could de-scope the system from 8×8 to 5×5 WFS subapertures and DM actuators. This takes the Strehl ratio back up to 50% for $V = 17$, although of course it can never beat the 8×8 in good conditions. We can immediately see the importance of reducing dome seeing to a bare minimum before attempting any common-user AO. The half arcsecond programme on the WHT and the UKIRT upgrades programme provide this essential pre-requisite.

Another crucial parameter is, of course, the timescale of seeing changes. This parameter is unfortunately less well-studied at our sites than the spatial coherence of seeing and until its better known we must ensure that our AO systems have sufficient maximum bandwidth.

The off-axis performance of AO systems is crucially dependent on the vertical distribution of the strength of turbulence as illustrated in figure 4. Off-axis performance determines not only the variation of image quality across the field but also the sky coverage for guide stars of a given magnitude. Again, remedial action is possible: where a dominant turbulent layer exists we can improve off-axis performance by moving the DM to an image of this layer. This is not wholly without cost, however,

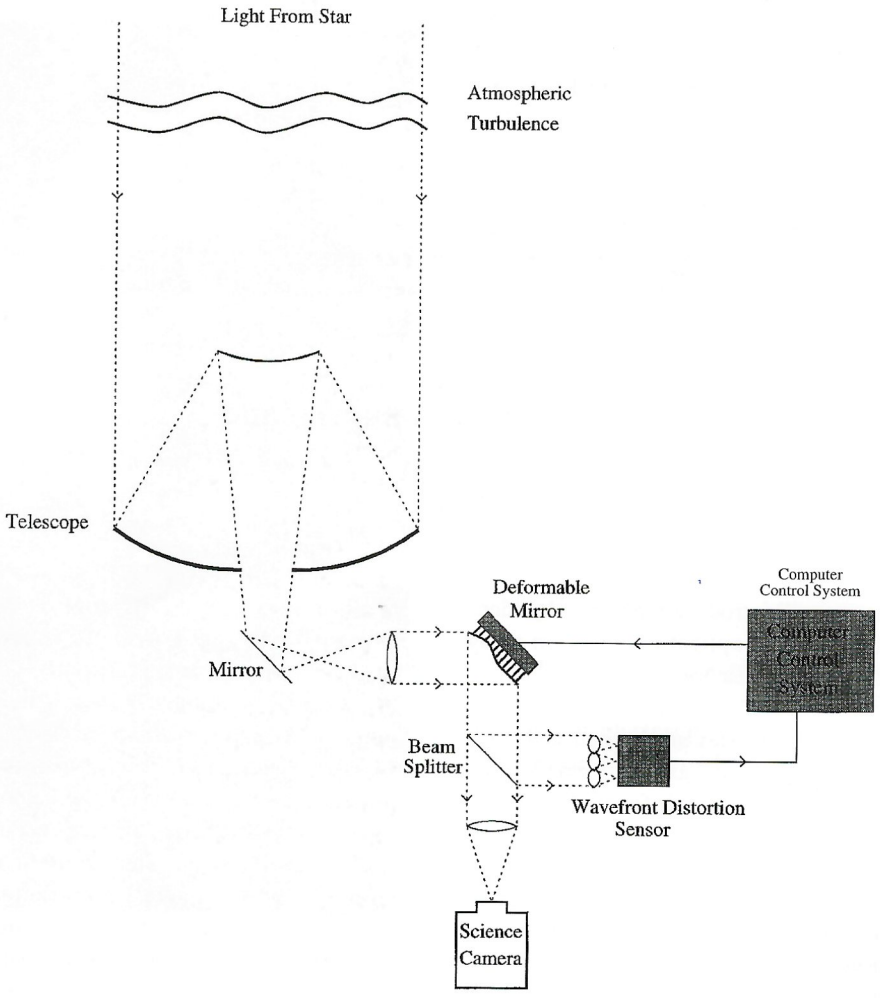

Fig. 3 – Simplified schematic of an adaptive optics system.

Anisoplanatism

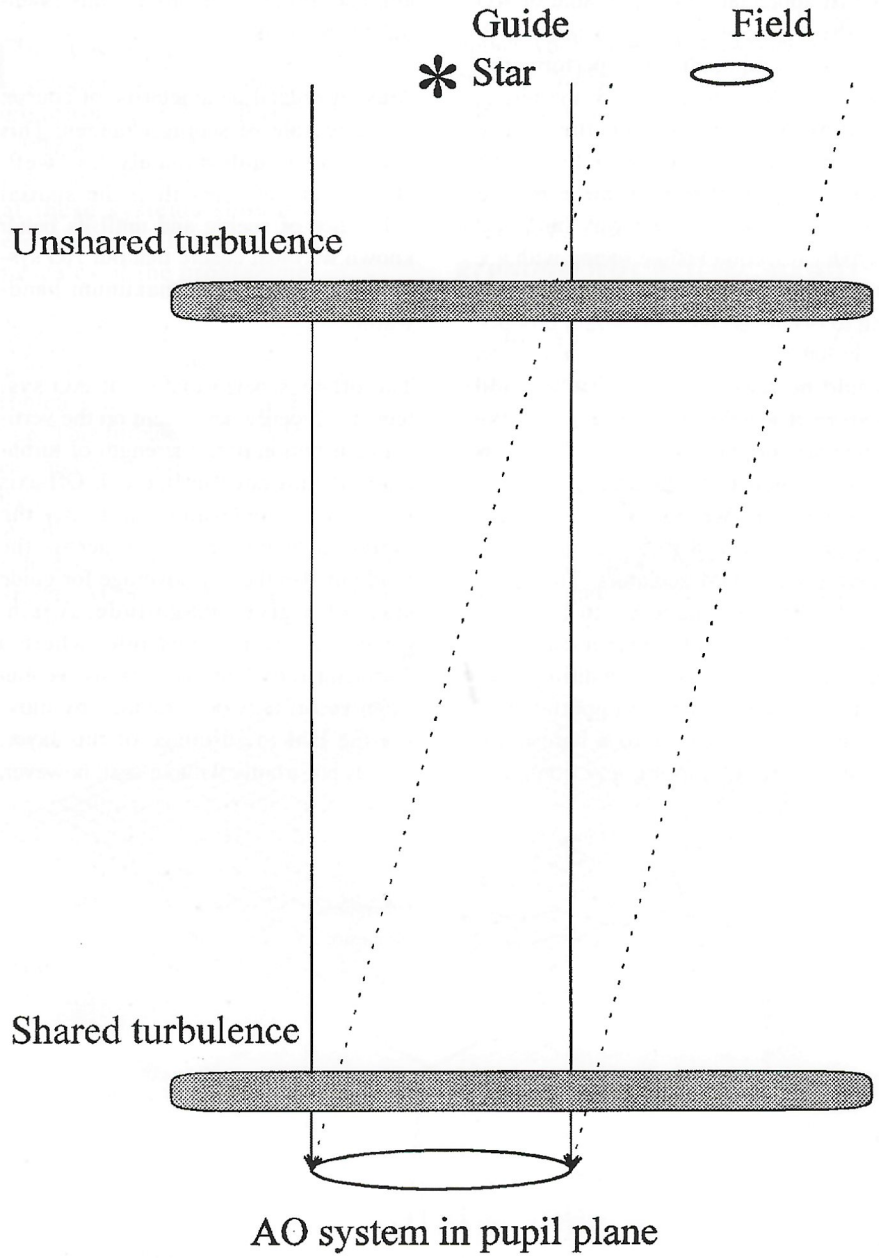

Fig. 4 – A schematic diagram illustrating the effects of the height of turbulence on an AO system conjugated to the telescope pupil. The turbulent layer which is not shared between the guide star and science target cannot be corrected at all. Intermediate layers receive a sheared, and therefore decorrelated, correction.

as we will introduce vignetting by moving the DM optical conjugation away from the telescope pupil. Statistics of the vertical distribution of turbulence at our observatories are limited and most predictions of off-axis performance and sky coverage are informed guesses. However we do have sufficient experience with experimental prototypes on La Palma and the modelling work of Charles Jenkins and Richard Wilson at RGO to know that AO is indeed very feasible at WHT (see figure 5 for an example field in M92 taken with Martini-2 at WHT GHRIL).

Finally we come to the effect of observational wavelength. We can expect good performance in the near-IR with natural guide stars but for most visible imaging, though not all spectroscopy, we will find sky coverage much reduced by the requirement for more actuators, shorter correction timescales and hence brighter guide stars. The problem is compounded by a smaller corrected field (the isoplanatic patch). The long-term remedy here is the use of laser guide beacons. These are powerful laser beams scattered from the upper atmosphere to produce artificial stars. They are, however, not without their drawbacks in a multi-telescope observatory.

A new approach to AO

The important feature that will make our common-user 4-metre AO systems different from previous prototypes will be the ability to adapt to most of these changing conditions and thereby provide high performance with high sky coverage throughout the year. This capability is being designed in from the start but the final implementation will require a programme of high speed wavefront measurements at both sites and a database of vertical turbulence distributions. Such site data are the essential prerequisites for programming the final AO systems to maintain the highest possible performance. The Joint Observatory Site Evaluation (JOSE-AO) programme has been set up to provide these data over the coming months. It will measure the AO-specific parameters at both sites and will also exploit the existing programmes on dome environment, free atmosphere seeing and meteorological monitoring.

The UPC (now USC) and the JSC have already agreed to the principle of time being made available in small but frequent slots for the JOSE-AO measurements. We ask for the cooperation of those whose observing will be slightly affected by this programme. The measurements obtained will eventually leading to significantly enhanced facilities for them in future.

We are also considering research and development programmes on laser-beacons and AO-optimised instrumentation to provide still wider exploitation of AO.

The AO programme timescales

The goal is to commission the funded common-user natural guide star (NGS) AO systems at the WHT and UKIRT in 1997 and 1998 respectively. However, we will not have to wait so long to get practical experience of near-IR AO. A more pragmatic, though much less advanced, near-IR AO system is already nearing completion. We will commence commissioning on the WHT GHRIL next February with a view to sharing it with the community as soon as possible

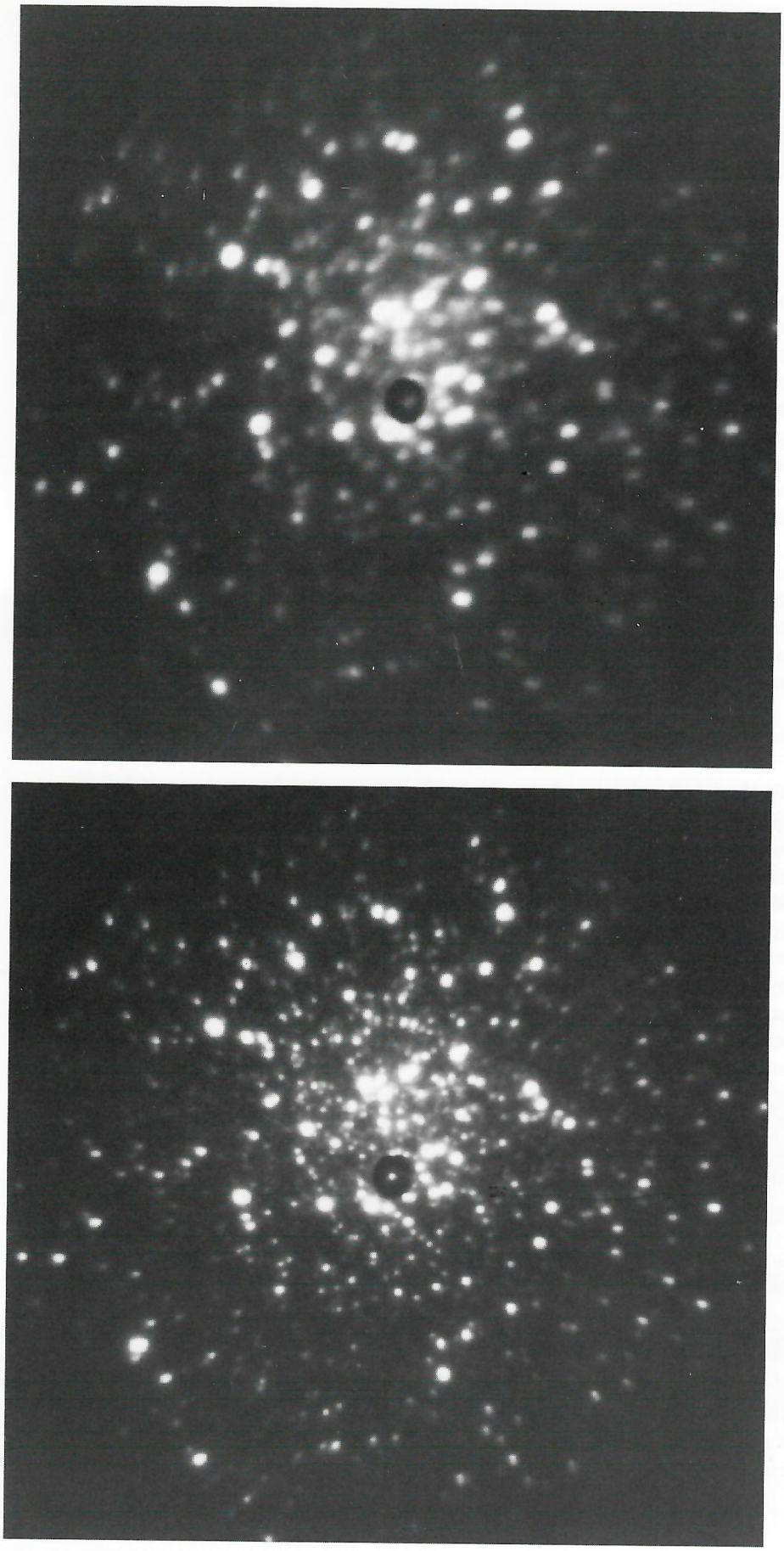

Fig. 5 – Before-and-after 50 second R band exposures with Martini-2 at WHT GHRIL. The corrected image FWHMs at the centre of the field are ~0.4 arcseconds.

in 1995. The AO system will be a refurbished Martini (Martini-3) which will employ a new Astromed CCD-based wavefront sensor implemented by the COAST group at MRAO, Cambridge. Although the AO system will not be truly common-user, the science instrument, WHIRCAM, will be a fully-fledged common-user IR camera which will be available at WHT GHRIL with or without AO. It is a UKIRT-type IRCAM with a 256 × 256 pixel 1 – 5 μm InSb array. WHIRCAM has been built remarkably quickly by a collaboration between Oxford University, led by Pat Roche, and the ROE. Measured performances of WHIRCAM/Martini-3 at GHRIL will be made available to the community as quickly as possible.

Contacts and communication

The main contacts for the UK AO Programme are: Programme Manager, Andy Longmore, ROE, **ajl@roe.ac.uk;** Project Scientist, Richard Myers, Durham, **r.m.myers@durham.ac.uk;** Programme Consultant, Ron Humphreys, Durham (part-time), **r.a.humphreys@durham.ac.uk.**

You can also join our mailbase listserver. To do this please send an email message as follows:-

To: **mailbase@mailbase.ac.uk**
Subj: anything
join ukao-info your-firstname your-lastname
stop

Please contact Richard Myers at Durham (tel: +44 91 374 2192) if you have any problems.

Acknowledgements

The AO simulations were drawn from work by Peter Doel, Durham. Pete used a turbulent phasescreen generator by Andreas Glindemann, MPIA.

Richard Myers, University of Durham,
Andy Longmore, ROE

ukirtinform

UKIRT News

The current phase of the primary mirror support upgrades work, which is seeing UKIRT closed for three weeks (17 October – 6 November), is proceeding very well. The work consisted of converting the existing 80 axial supports of the primary into three separately controllable sectors, installing the hardware for twelve individually controllable axial supports around the outer edge of the mirror, and machining in preparation for the installation of a primary mirror cooling system. Night-time image quality tests began on 31 October; initial reports are good.

The UKIRT primary mirror is now being cleaned using CO_2 'snow'. Previously, N_2 gas and/or washing with water were used. In the new technique, gaseous CO_2 from a standard cylinder comes out through a special nozzle, cools, and forms pellets of solid CO_2, These are very effective at loosening dust from the mirror surface without damaging the surface. The appearance of the mirror surface and preliminary checks of the telescope emissivity suggest that the new technique works quite well.

In late October, CGS4 was transported to Hilo. Work on the array upgrade (58 × 62 to 256 × 256) was scheduled to begin on 7 November. Mechanical upgrades will follow in early 1995. It is expected that CGS4 will be recommissioned in April 1995. In the few weeks prior to the removal of CGS4, significant improvements to the CGS4 control and data reduction software and displays were implemented. These have been well received by recent CGS4 users.

Tom Geballe, JAC

UKIRTSERV News

The UKIRT service observing programme presents an opportunity for astronomers to have a short observational project (less than two hours including overheads) carried out by UKIRT staff astronomers. Service nights are scheduled on average every month. The deadline for receipt of applications is approximately four weeks before the run; applications received are refereed in the intervening weeks. Typical projects included long term monitoring of variable sources, observations of targets of opportunity, short self-contained programmes or observations required to complete a programme started during PATT allocated observing time. If you require any further information, or wish to be added to the mailing list, please contact **UKIRTSERV@roe.ac.uk**. The successful operation of UKIRTSERV relies heavily on the efforts of the referees and observers, whose invaluable help I am pleased to acknowledge.

As the VAX is no longer in use at the Royal Observatory, UKIRTSERV has made the transition to UNIX, and may now be contacted as **UKIRTSERV@roe.ac.uk**. UKIRTSERV also has a revamped entry in the ROE Home Page of the World Wide Web (**http://www.roe.ac.uk/ukirt/ukirtserv.html**), which gives details on the aims and operation of UKIRTSERV, as well as allowing the application form to be copied.

Users may already know that CGS4 is currently unavailable as it being upgraded. The 58 × 62 pixel array is being replaced with a 256 × 256 pixel array giving increased sensitivity thanks to lower noise performance, smaller pixels and increased spectral coverage. Astronomers with current CGS4 projects are invited to resubmit their applications with the observations tailored to the new chip. Sensitivities are available on the World Wide Web. We anticipate that CGS4 will be scheduled for service observations again in the Spring.

Suzanne Ramsay, ROE

Service Schedule for Semester 94B

The UKIRT Service runs for Semester 94B are provisionally scheduled as follows. Many nights are shared with AIC/Engineering and so dates, deadlines and instruments may change in subsequent reminders. Accepted observations remain in the queue, so please apply as early as possible to maximise scheduling flexibility.

Date	Instruments	Deadline (Noon UT)
Dec 13	IRCAM3	Nov 26
Jan 10 – 11	IRCAM3, UKT8, CGS3	Dec 15
Jan 12	IRCAM3, UKT8, CGS3 (2nd half)	Dec 15
Jan 13	CGS3 (2nd half)	Dec 15

Further Experiments with Shift-and-Add Imaging

The new UKIRT imager IRCAM3 (see *Spectrum* No 2, June 1994, page 4) offers pixel scales up to 0.057 arcseconds per pixel, sufficient for Nyquist sampling of diffraction-limited images on UKIRT at 2.2 μm. The ALICE electronics allow very rapid readout of data for coadding in memory, when each frame can be automatically shifted to match its brightest pixel with that of the coadded data array: a 128 × 128 subarray can be read out at up to ~30 Hz. The 'brightest pixel' matching tehnique exploits the single-speckle structure of NIR images and when the seeing is good enough, which appears to be quite commonly the case, produces dramatic images with a diffraction-limited core.

The main variables affecting performance in Shift-and-Add (SAA) mode are the readout frequency (which determines on-chip exposure), pixel size, wavelength and seeing. On-chip exposure is especially important for sensitivity, as the array has about 30 electrons read noise. In the *K*-band, on exposures of less than a couple of seconds, this noise is dominant and S/N varies linearly with on-chip exposure time. Thus a 3 s on-chip *K*-band exposure may have background photon noise at about 50 electrons per pixel but a SAA version with the same total exposure, but made up of 75 on-chip frames each of 40 ms, will suffer the equivalent of 2250 electrons noise per pixel, giving a reduction in S/N by a factor of ~45.

For this reason when we carried out SAA test observations at *K* (2.2 μm) on 9 August 1994 we particularly investigated the effects on spatial resolution of the readout frequency. Sets of images of bright stars were taken at readout rates of 25, 12.5, 8.3, 5 and 2 Hz, as well as uncorrected DC images using direct, unshifted coaddition, to measure the 'normal' seeing. Each image totalled 80 s exposure time, so that (*eg*) the 25 Hz images each comprised 2000 exposures, each of 40 ms on-chip. Pixel scales of 0.143 arcseconds and 0.057 arcseconds were used.

The table gives results of part of the run, measurements of HD 225023 (K = 6.9) using the ×2 and ×5 magnifiers, in the form of an approximate Strehl ratio (of the observed peak intensity to that in a perfect image at the same wavelength and pixel scale), and a FWHM derived from a fitted Gaussian. The latter is a generally poor representation of the true quality of an image if the Strehl is above 15%, since the brightest parts of such images are dominated by a central, diffraction-like spike.

SDEV is the population standard deviation, indicating how consistent the image structure is over a period of tens of minutes (the time required to obtain a set of 6 or 8 images).

In all cases but one, the faster-sampled images are better both in Strehl and in FWHM. The dependence on frequency, however, is not constant, but apparently varies with the seeing. The change from ×2 to ×5 magnifier also appeared to produce an improvement in image quality.

As explained above, one wants to use the longest on-chip exposures compatible with good spatial resolution. So it is nice to note that the 25 Hz and 5 Hz runs with the ×5 magnifier differ in Strehl ratio by a factor of less than 2. At 5 Hz the S/N would be a factor of 5 higher, while S/N is proportional to Strehl ratio (at least insofar as the central spike is concerned), so this implies that a small sacrifice in spatial resolution led to a gain in S/N (equivalently of limiting brightness) by a factor of 2.6. (A repeat of the 5 Hz measurements on a K = 10.3 star showed no loss of image quality.)

HST	Freq (Hz)	Strehl (%)	SDEV(%)	FWHM (arcseconds)	SDEV (arcseconds)
Pixel FOV = 0.143 arcseconds					
02:23	25	14.7	1.3	0.24	0.02
02:33	12.5	13.2	0.7	0.27	0.02
02:45	8.3	11.4	1.1	0.28	0.02
02:57	5	11.6	1.5	0.35	0.02
03:08	2	7.1	0.3	0.54	0.01
03:21	DC	6.0	0.2	0.60	0.01
03:32	25	22.9	1.8	(0.14	0.01)
Pixel FOV = 0.057 arcseconds					
04:06	25	30.0	3.4		
04:19	12.5	25.4	2.1		
04:33	8.3	18.6	5.2?		
04:44	5	16.5	2.2		
04:53	2	10.6	0.8	0.24	0.04
05:05	DC	6.0	0.4	0.43	0.04

It's sometimes nice to come out ahead of this sort of game: before these experiments we feared that reduced readout frequency would degrade the image quality more severely than the resulting gain in sensitivity would warrant. However we will still need a lot more experience before a recipe for optimised performance can be assembled!

Images with spectacular spatial resolution (FWHM of order 0.15 arcseconds) can currently be obtained at UKIRT by using real-time shift-and-add, even though the telescope enhancements are not yet complete. Further optical improvements are planned and should increase the fraction of the time when this is possible and the amount of power in the central spike. There appears to be lots of room for beneficial tradeoffs of image quality against sampling frequency. While we still have a lot to learn, the images of recently-formed binaries taken by Colin Aspin, shown on page 6 in this issue, illustrate that the method is already yielding scientific returns.

Tim Hawarden, JAC

CGS4 Data Reduction News

Users are reminded that there is a recent (July) VMS version of CGS4DR (version 2.0-0) available. If you wish to use CGS4DR to reduce data taken since June 1994, which are in NDF format, you must have this latest version of CGS4DR. This version of CGS4DR can reduce both the old (DST) and the new format CGS4 files. The Unix version of CGS4DR will also be able to handle both file formats.

Good progress is being made towards providing a version of CGS4DR which will run under Unix, and we still hope to have a version of this available by the end of the year. This timescale assumes that we do not run into any unexpected problems and that the port of a few outstanding ICL and Unix ADAM items is completed and bug free. *We recommend that if you have an urgent need to reduce CGS4 data in the December – January period, you request that one of your VAX Stations be left operational for this purpose.* We will not release the Unix CGS4DR until it has been demonstrated to work at the JAC. The first release may be a minimal version which does not include some purely engineering features and some manual options which can be handled by other software such as Figaro.

Gillian Wright, JAC

UKIRT_INFORM moves to the World Wide Web

As of the beginning of Semester 95A, the old UKIRT_INFORM directories at ROE and in Hawaii will cease to exist and all of the UKIRT_INFORM will be available on the World Wide Web (WWW) only. At present this WWW version is being configured and tested. The old UKIRT_INFORM is no longer being updated, so only the WWW UKIRT_INFORM will reflect recent changes.

Access to the WWW UKIRT_INFORM can be obtained using a variety of hypertext browsers, but the MOSAIC (mouse-driven; Xwindows interface) and LYNX (text-only interface) browsers are highly recommended. The WWW UKIRT_INFORM server has the following URL: **http://www.jach.hawaii.edu/UKIRT/Inform/www/inform.html**

The WWW UKIRT_INFORM may also be accessed from UKIRT's home page which has the following URL: **http://www.jach.hawaii.edu/UKIRT/home.html**

Once there, click on UKIRT_INFORM and follow the links to the information you require or put in the URL for the Joint Astronomy Centre Hilo Home Page: **http://www.jach.hawaii.edu/**. Click on the United Kingdom Infrared Telescope and make your choice.

UKIRT_INFORM covers a variety of information, including: an introduction to UKIRT; PATT proposal form; telescope time allocations for recent semesters; accommodation request form for visiting Hawaii; observer report form; service observing (dates, instruments, appplication form); documentation on UKIRT instruments; data reduction; sensitivities, calibration; news items.

Any questions, problems, or suggestions regarding the UKIRT_INFORM are welcome. While the new UKIRT_INFORM is being developed your patience will be appreciated.

Dolores Walther, JAC

The Green Flash over Teide

I think it was Professor Rod Davies who first asked me to join him on the edge of the caldera beside the JKT before breakfast on a cold January morning to watch the sun rising. From there one has a clear view of the black outline of the island of Tenerife and its majestic peak, Teide, about 70 miles to the E.S.E. of La Palma. He told me to keep my eyes trained on a particular place on the outline of Teide. It was a crisp, clear morning and great shafts of sunlight were streaming on either side of Teide: the Sun was already above the sea horizon but it was hidden by Teide. Suddenly I saw a brilliant, piercing blue-green diamond of light near the point I had been watching. It lasted for about a second before being obliterated by the blinding red limb of the Sun.

I never forgot that stunning spectacle and on my subsequent trips to La Palma in January I have often witnessed the same phenomena. Last January I had the pleasure of showing Brian Boyle the so-called 'green flash' and he too became an avid observer of the phenomenon. He suggested that I should write a piece for *Spectrum* to bring it to the attention of others who visit the Roque between November and January.

The 'green flash' is caused by the prism-like action of the atmosphere which disperses light of different wavelengths into a spectrum. The greatest dispersion of sunlight occurs near the horizon where the rays traverse the longest path in the atmosphere. The blue end of the spectrum is refracted most, and the red least. Figure 1 shows a schematic side view of the Sun rising behind Teide as viewed from the Roque de los Muchachos on La Palma. A blue ray of light from the upper limb of the Sun is refracted by the atmosphere and skims over Teide to arrive at the observer on the Roque. The red ray, which is refracted less, passes above the observer's head. (The dispersion is greatly exaggerated in the figure for illustrative purposes.) As the Sun rises, Teide acts like a pivot, with the spectrum sweeping down over the observer who sees the blue-green image of the uppermost tip of the Sun briefly before the dominant red-yellow part floods the observer's vision.

Spectacular views of the 'green flash' phenomenon can be seen at sunrise from the Roque de los Muchachos between November and January.

Of course, it is not essential to have Teide between the Sun and the observer: the horizon provided by the curvature of the Earth can also act as a mask. However, Teide offers several advantages over the sea-level horizon. Often there is cloud or lanes of dust near sea-level. Teide is normally above the inversion layer and most of the dust in the atmosphere. It provides a very sharp edge against the sky, in contrast to the hazy horizon at sea-level. The fact that the observer is on a mountain top means that he or she too is usually above the clouds and dust.

Islands separated by sea (they usually are!) are also preferable to an intervening land mass because there is less chance of the smooth laminar structure of the atmosphere being disrupted by turbulence which confuses the prism-like action of the atmosphere.

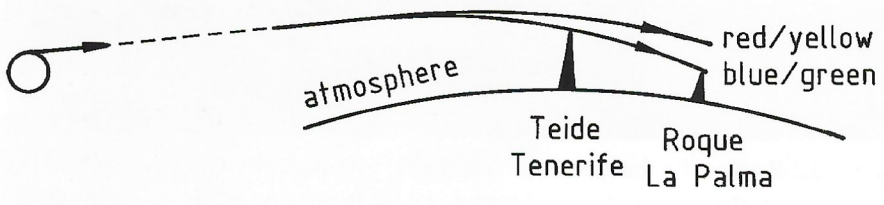

Fig. 1 – Origin of the 'green flash'.

Another physical effect which has a bearing upon the visibility of the 'green flash' is the preferential scattering of blue light in the atmosphere. This diminishes the amount of direct blue light reaching the observer and hence the 'flash' is usually green in colour rather than blue. Here again, the mountain sites favour the possibility of seeing the blue part of the spectrum because the atmosphere is less dense than at sea-level and there is less scattering of the blue light. Less density also means less dispersion though. However, the long path length of the rays through the atmosphere produces sufficient dispersion to separate out the blue part of the spectrum. On several favourable occasions I have indeed seen the blue part of the spectrum preceding the green.

Unfortunately, there is no suitably placed island to the west of La Palma to produce a silhouette corresponding to Teide in the east. Nevertheless, using the sea-level horizon I have often witnessed the tip of the Sun turn green just before setting. In my opinion this phenomenon would not be described as a 'flash' and it is not nearly as arresting as the blue-green flash at sunrise over Teide.

Figure 2 is a scale drawing of the outline of Teide as seen from the Roque de los Muchachos, showing a few of the most salient features and the dates when the Sun rises behind them. The Sun reaches its most extreme southerly azimuth of sunrise at the winter solstice on 22 December. The times of sunrise are given to the nearest minute.

The progress of sunrise along the outline of Teide provides an effective way of determining the date of the winter solstice, and it is tempting to speculate that the Guanche inhabitants of La Palma used it as a calendar. I may have been misled in this speculation by my interest in the megalithic culture in France and the British Isles which certainly used the progress of sunrise and sunset along the horizon for calendarial and ritualistic purposes.

In conclusion, I encourage astronomers visiting the Roque between the third

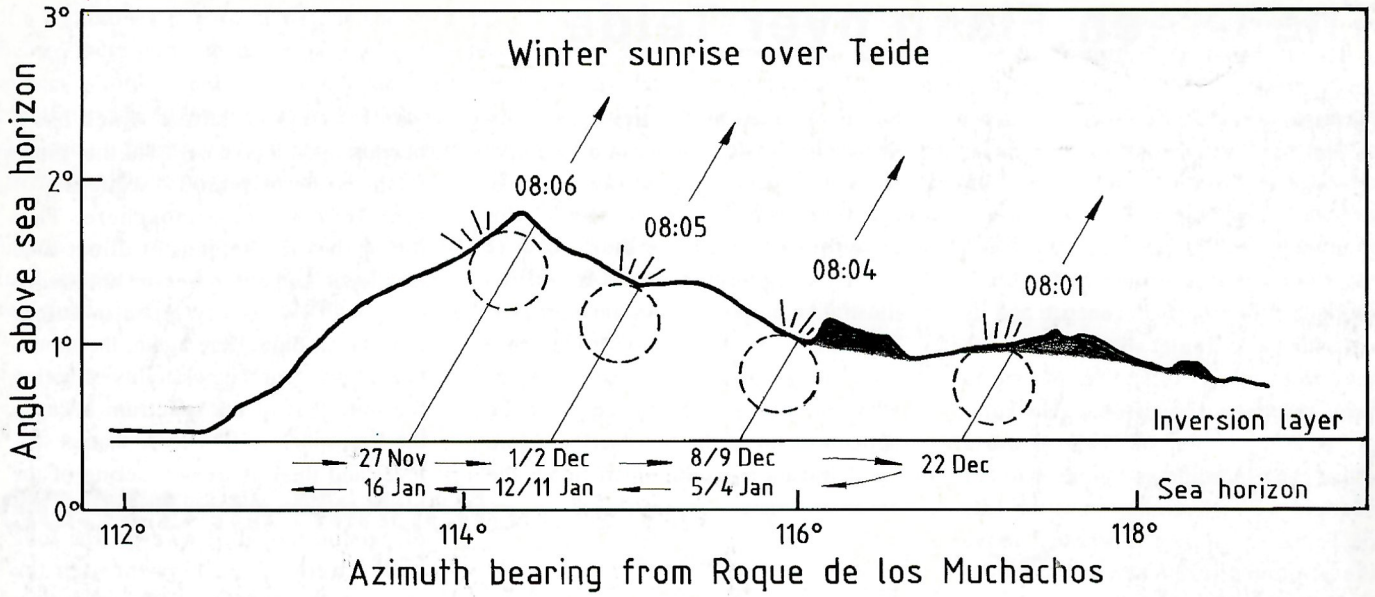

Fig. 2 – Winter sunrise over Teide.

week in November and the third week in January to leave their flat-fielding for five minutes and make their way to the rim of the caldera where a wonder of nature awaits them. I thank Derek Jones for providing the outline of Teide and Bernard Yallop for checking the azimuths and my observed times of sunrise given in Figure 2. I am grateful to Janet Wicks for drawing the figures.

Leslie Morrison, RGO

Forest Fires on La Palma

Juan Sanchidrian, *El Dia*

Serious forest fires approached the Observatorio del Roque de los Muchachos on August 27 (above, viewed from the west) after raging on La Palma for three weeks and affecting some 10% of the pine forests. Thanks in part to all-night fire-fighting by Observatory staff, the fire did not damage any of the telescope buildings, although the German gamma-ray experiment lower down the mountain (hidden by smoke in the picture) suffered the loss of a small part of its array. The nearby Residencia had a narrow escape, with flames approaching within metres of the walls.